Politecnico di Torino

POLITECNICO DI TORINO

Dipartimento di Ingegneria Meccanica ed Aerospaziale

Corso di Laurea Magistrale in Ingegneria Biomedica

Biomechanical analysis of use of porous meta-diaphyseal custom-made cones in knee revision surgery

Relatore
Prof. Cecilia Surace

Candidata
Marika Padalino

Supervisore
Prof. Bernardo Innocenti

A.A. 2022/2023
Ottobre 2023

Alla mia cara nonna Maria,
presente, anche se non fisicamente,
in tutto quello che faccio,
e sempre lo sarà.

I. Contents

II. List of figures

III. List of tables

Abstract

In many cases, traditional revision (TR) implant may be an effective solution to be used after primary TKA. However, it does not cover the full range of clinical possibilities, especially in patients with multiple revisions presenting an extremely weak bone and a variable geometry. Therefore, custom-made metaphyseal titanium porous cones were developed as an alternative to amputation in patients with severely pathological bone conditions.

The aim of the study is to evaluate whether this innovative implant is able to restore patient's ability to perform simple daily activities, in comparison with TR.

The performances of implant were compared with TKA with cementless press-fit stems and cemented stems and using a large resection prosthesis with cemented stems. These techniques were simulated by FEA and daily activities as full-extension and chair-rise configuration were analyzed with applied static force. Stress patterns in the interface regions between prosthesis and bone and risk of fracture in the bone were extracted and compared.

Biomechanical results demonstrate that the use of custom-made devices can be considered a viable option to manage the patient's bone loss because the bone stress is more homogeneously distributed than stress induced by the other three techniques, where is more concentrated in specific regions.

Sommario

In molti casi, l'impianto di revisione tradizionale (TR) può rappresentare una soluzione efficace da utilizzare dopo l'artroplastica totale del ginocchio primaria. Tuttavia, non copre l'intero spettro delle possibilità cliniche, specialmente nei pazienti sottoposti a molteplici revisioni che presentano un osso estremamente debole e una geometria variabile. Pertanto, sono stati sviluppati coni porosi in titanio metafisario su misura come alternativa all'amputazione nei pazienti con condizioni ossee gravemente patologiche.

Lo scopo dello studio è valutare se questo impianto innovativo sia in grado di ripristinare la capacità del paziente di svolgere semplici attività quotidiane, confrontandolo con il TR.

Le prestazioni dell'impianto sono state confrontate con l'artroplastica totale del ginocchio con steli press-fit senza cemento, steli cementati e l'uso di una protesi di grande resezione con steli cementati. Queste tecniche sono state simulate tramite analisi agli elementi finiti (FEA) e le attività quotidiane come l'estensione completa del ginocchio e il sollevamento da una sedia sono state analizzate con l'applicazione di una forza statica. Sono stati estratti e confrontati i modelli di stress nelle regioni di interfaccia tra la protesi e l'osso e il rischio di frattura nell'osso.

I risultati biomeccanici dimostrano che l'uso di dispositivi personalizzati può essere considerato un'opzione valida per gestire la perdita ossea del paziente poiché lo stress osseo è distribuito in modo più omogeneo rispetto allo stress indotto dalle altre tre tecniche, dove è più concentrato in regioni specifiche.

Chapter 1

Introduction

1.1. The native knee joint

The knee is the largest joint in the human body and the most complex. It is the intermediate joint of the lower limb and allows movement between the femur, tibia and patella.

The anatomy of the knee (Figure 1.1) is composed of four bones: femur (thigh bone), tibia (shin bone), patella (kneecap) and fibula (calf bone) [1].

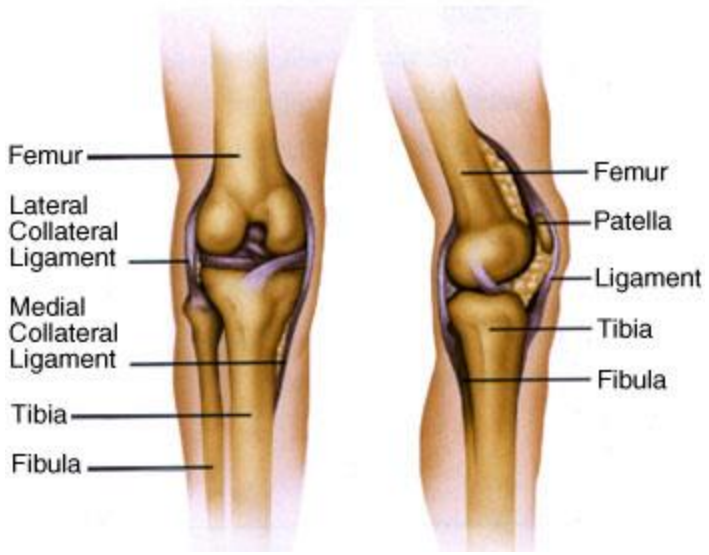

Figure 1.1: The anatomy of the knee.

The peculiarity of the knee is that it must be very stable when standing, which means that the joint does not move but is blocked by various structures, whereas when walking, running or changing direction, the knee is continuously subject to flexion-extension. So, it is an anatomical structure that has to respond to two conflicting needs at different times [2].

In fact, although the anatomy of the knee joint varies from patient to patient, the complex function of the knee joint is the result of two joints that make up the knee: the tibiofemoral joint (TF) and the patellofemoral joint (PF) [1,3].

- The Femur is the longest and most voluminous bone of the leg, located in the thigh. The distal epiphysis of the femur has two oblong, rounded prominences called the lateral and medial condyle (Figure 1.2). Their postero-inferior surface articulates with the proximal aspect of the tibia and the medial and lateral menisci of the knee to form the TF joint [4].

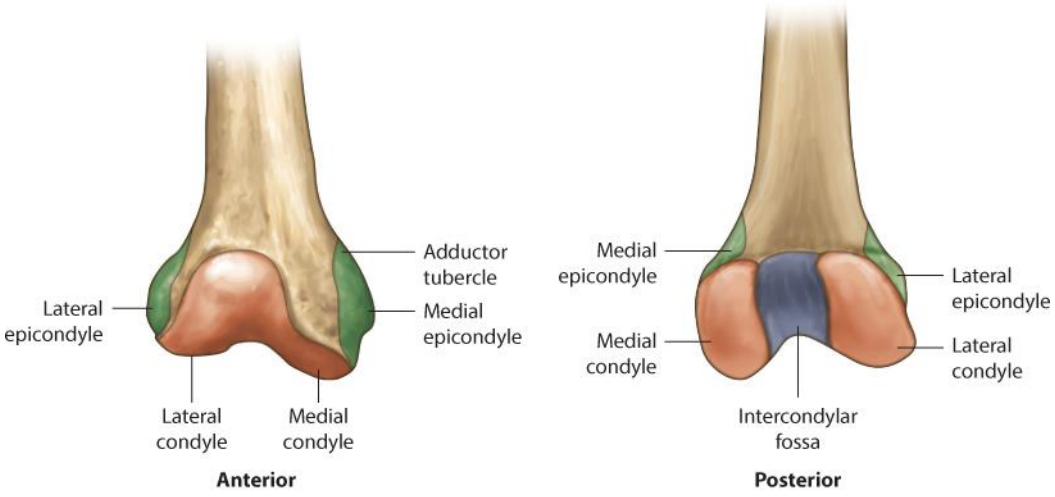

Figure 1.2: Anterior and Posterior proximal femur.

Both the medial and lateral condyles have a convex protuberance, called the medial and lateral epicondyle respectively (Figure 1.2), which is the insertion site of the ligaments and tendons [4]. Furthermore, looking posteriorly, between the two condyles there is an intercondylar fossa, an attachment area of the anterior and posterior cruciate ligaments, while anteriorly we can see, in Figure 1.3, a femoral trochlear groove, which is a smooth, shallow articular depression that guides the patella into the PF joint [5].

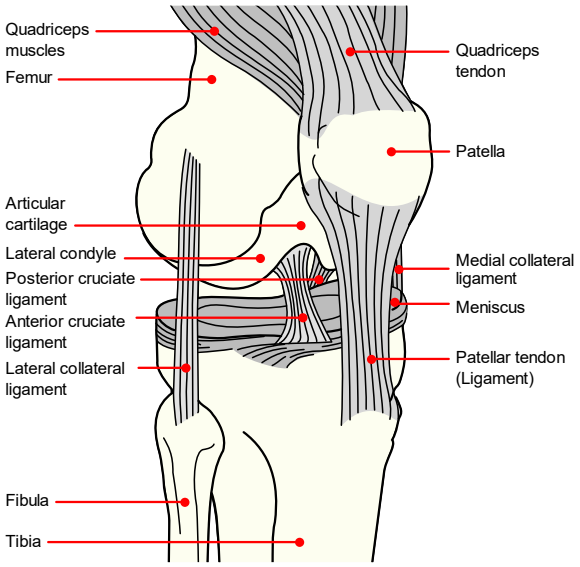

Figure 1.3: The ligaments and bones involved in knee joint.

There are two long bones located in the lower leg: the tibia and the fibula.

- The Tibia, commonly referred to as the shin bone, is situated in the lower leg, providing support for the femur. It ranks as the second-largest and strongest bone in the human body. Positioned along the inner side of the leg (medial), it extends from the knee joint down to the ankle. The upper end of the tibia features two plateau-like surfaces, known as the medial and lateral tibial condyles, separated by an intercondylar eminence housing the medial and lateral tibial spines (Figure 1.4 and Figure 1.5-A). Each tibial condyle's superior section consists of an oval-shaped articular surface covered with hyaline cartilage, accommodating the corresponding femoral condyle [4]. In the coronal plane, both tibial plateaus exhibit concavity, whereas in the sagittal plane, only the medial one is concave, with the lateral one being convex. This asymmetry enhances the lateral mobility of the knee joint. Additionally, the medial plateau boasts a larger and thicker articular surface compared to its lateral counterpart.

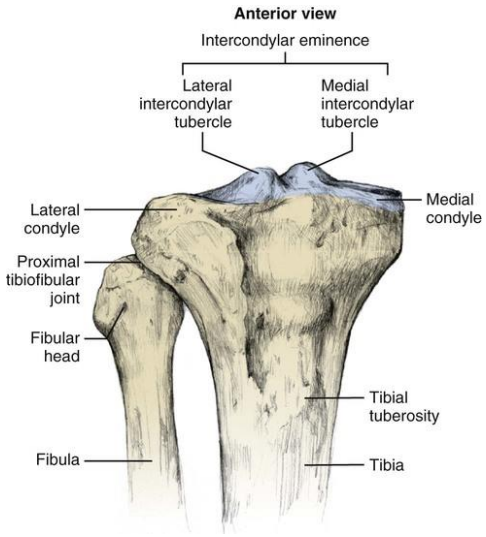

Figure 1.4: The anatomy of the proximal tibia.

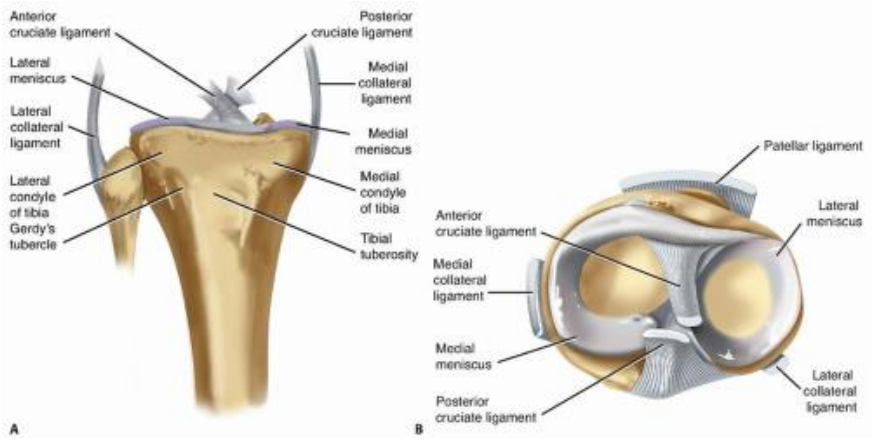

Figure 1.5: The ligaments of the tibia (A) and Superior view of tibial plateau (B).

Adjacent to the lateral aspect of the tibia, both proximally and distally, lies the fibula.

- The Fibula, a slender and elongated bone, runs parallel to and alongside the tibia, forming articulations with it at its upper and lower ends. This bone plays a vital role as an attachment site for muscles and the lateral collateral ligament. In comparison to the tibia, it is notably smaller and thinner, but it serves as a significant anchor point for various muscular attachments. Working in tandem, the tibia and fibula cooperate to provide stability to the ankle and support the muscles of the lower leg [5].

- The Patella is a rigid, triangular bone situated at the front of the knee joint, positioned in the intercondylar notch and firmly anchored within the tendon of the quadriceps femoris muscle above and the patella tendon below. Its posterior surface can contain as many as seven facets, covered with cartilage, with three on each side, engaging respectively with the medial and lateral femoral condyles [4]. During knee movement, the patella smoothly glides within a groove. It starts above the trochlear groove when the knee is fully extended, and as the knee flexes to around 20°, the patella aligns itself with the trochlear groove. By approximately 40° of flexion, the patella should be fully seated within the trochlea [5,6]. The patella serves a crucial biomechanical role by transmitting tensile forces generated by the quadriceps to the patellar tendon (PT) and the tibia, while also extending the lever arm length of the extensor mechanism throughout knee flexion. Additionally, it acts as a protective shield for the distal part of the femur, guards the quadriceps against frictional wear, and reduces sagittal shear stress on the knee joint.

To facilitate smooth and nearly frictionless movement, the patella features a layer of cartilage on its articulating surface, ensuring efficient pulley-like function. Similarly, the femur and tibia also possess cartilage layers on their articular surfaces, guaranteeing seamless sliding and providing shock absorption [7].

Situated between each femoral condyle and the underlying tibial plateau are two semilunar cartilages known as menisci (Figure 1.5-B) [7]. These menisci serve the dual purpose of restoring alignment between the bony surfaces and providing cushioning effects.

In addition to cartilage, a crucial component of the soft tissue in the knee includes ligaments and tendons, which, in collaboration with muscles, play a vital role in supporting the knee and regulating its stability (Figure 1.3) [5]. Within the TF (tibiofemoral) joint, the relevant ligaments encompass the

anterior cruciate ligament (ACL), posterior cruciate ligament (PCL), medial collateral ligament (MCL), and lateral collateral ligament (LCL) [1]. In the PF (patellofemoral) joint, key ligaments consist of the patellar tendon (PT)[5,8], medial patellofemoral ligament (MPFL) [5], and lateral retinaculum.

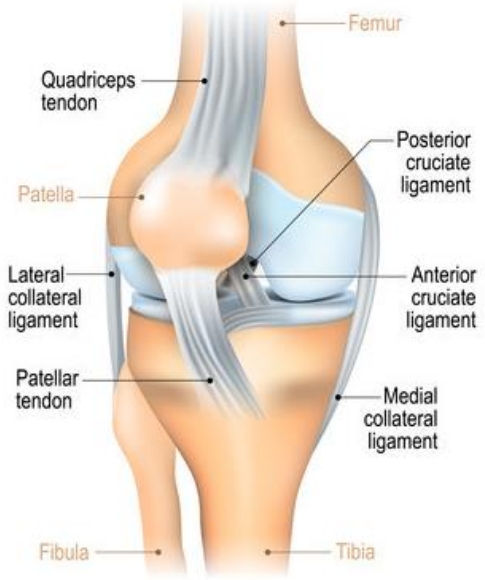

Figure 1.6: The collateral and cruciate ligaments.

Both sets of collateral ligaments (Figure 1.6) contribute to medial-lateral stability by preventing side-to-side movement of the knee joint. Furthermore, in cases of cruciate ligament tears, the LCL and MCL serve as secondary constraints to limit anterior and posterior translation of the tibia [4].

Instead, the cruciate ligaments (Figure 1.6) are categorized based on their attachment to the tibia as ACL and PCL: the ACL is affixed to the posterior surface of the medial aspect of the lateral femoral condyle, then descends inferiorly, intersecting with the path of the PCL, before attaching anteriorly to the tibia; Conversely, the PCL attaches to the anterior aspect of the lateral surface of the medial femoral condyle and inserts distally on the posterior surface of the tibia[1]. These cruciate ligaments play a pivotal role in maintaining joint stability and preventing anterior-posterior displacement. To illustrate, the ACL limits excessive forward displacement of the tibia relative to the femur, while the PCL performs the same function but in the opposite direction. This is of paramount importance, as

excessive displacements would necessitate the generation of increased muscular force to maintain equilibrium.

Additionally, both cruciate ligaments influence joint motion during passive movement, and their sensory endings contribute to the vital proprioceptive function.

Concerning the patella, the MPFL (Figure 1.7) serves as a critical static stabilizer, particularly when the knee is fully extended. Research indicates that it is the primary restraint against lateral patellar movement between 0 and 30 degrees of knee flexion [5].

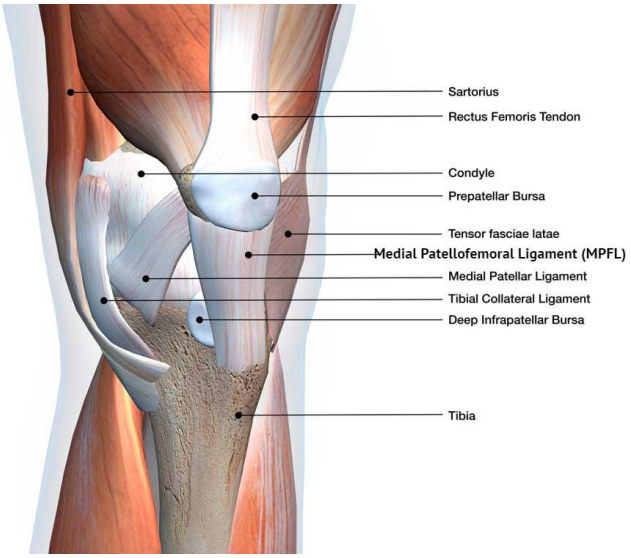

Figure 1.7: The MPFL.

The PT (Figure 1.3) functions as a connection between the patella and the tibial tubercle and is often referred to as a tendon since it extends from the quadriceps muscle. It facilitates the transmission of high tensile loads from the quadriceps muscle to the tibia while maintaining a consistent distance between the patella and tibia.

There are two primary sets of muscles that operate on the knee joint: the knee extensors, which include the quadriceps femoris, and the knee flexors, represented by the hamstrings. The quadriceps femoris, depicted in Figure 1.7, stands as the most robust muscle in the human body and stretches along the front compartment of the femur [5]. It comprises four distinct sections: vastus

medialis, vastus lateralis, vastus intermedius, and rectus femoris. These sections converge above the patella to form the quadriceps femoris tendon, which connects to the start of the patellar tendon (PT). Contraction of this muscle group facilitates leg extension at the knee joint and plays a pivotal role in activities such as walking, squatting, running, and jumping.

On the other hand, the hamstrings constitute a trio of muscles that act as antagonists to the quadriceps. They extend along the rear surface of the femur and can be categorized into medial hamstrings, which include the semitendinosus and semimembranosus, and lateral hamstrings, represented by the biceps femoris. These muscles are predominantly bi-articulate, as they perform both knee flexion and hip extension [5].

1.1.1. Knee joint biomechanics

As already explained, the knee joint is a structure with two articulations.

Specifically, the tibiofemoral joint is not a simple hinge joint but has a spiral or helical movement. Six degrees of movement are allowed (Figure 1.8), three of translation (anterior-posterior, medial-lateral, and inferior-superior) and three of rotation (flexion-extension, internal-external rotation, and adduction-abduction)[9].

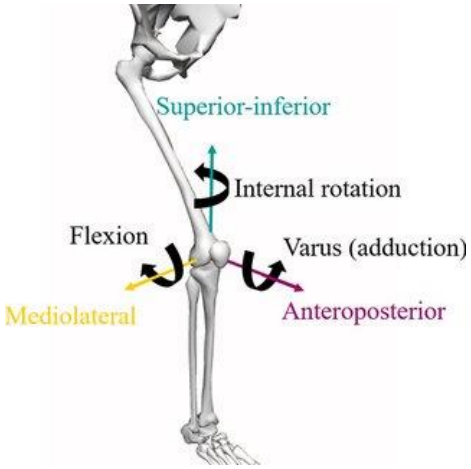

Figure 1.8: Six degrees of movement of knee joint.

These movements are determined by the sliding of the articular surfaces of the tibia and femur and the orientation of the four main ligaments of the knee (ACL, PCL, LCL and MCL).

In particular, the movement of flexion and extension is the widest and most important, while the other movements are very limited. The flexion movement can be active or passive and depends on the position of the hip (Figure 1.9). During active flexion, the knee can reach 140° with the hip flexed and 120° if the hip is extended (less because the force of the hip muscles is already being used, leaving less for the knee); whereas passively, it can reach 160°. During the extension movement, passive values are limited to 5-10° from the reference position. The typical range of motion during walking for flexion-extension is mostly rolling (15-20°)[10,11,12].

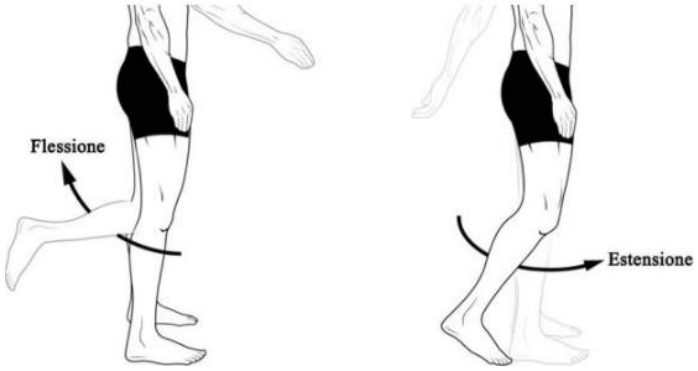

Figure 1.9: The flexion/extension movement of the knee joint.

To ensure flexion without slipping, a combination of rotation and sliding movements of the femur on the tibia is required. Flexion is associated with internal rotation of the tibia, while extension is associated with external rotation of the tibia relative to the femur. This external rotation provides greater stability to the knee.

The rotation of the leg around its longitudinal axis can only occur when the knee is flexed, at approximately 90° (Figure 1.10). When the hip is at 90°, internal rotation ranges from 0° to about 30°, and external rotation ranges from 0° to about 40°. If the hip is extended, internal rotation ranges from 0° to about 45-50°, and external rotation ranges from 0° to about 30-35° [4,12].

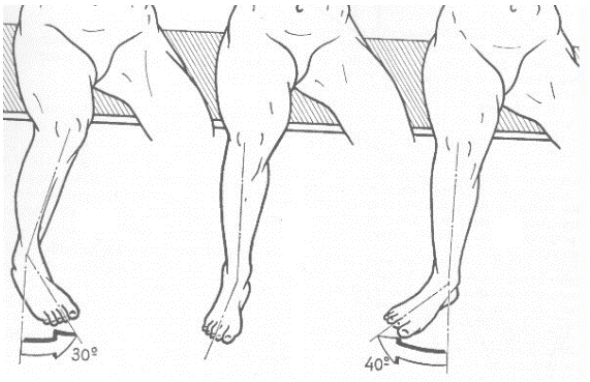

Figure 1.10: The internal/external rotation of the knee joint.

In the reference position used for assessing internal-external rotation, the leg exhibits a brief passive movement of adduction-abduction, but this completely disappears when the knee is extended. Specifically, the leg moves towards the body's plane of symmetry, performing a motion in the frontal plane that can be seen as an adduction movement. The typical value of this angle is 10-15° [4].

On the other hand, the patellofemoral joint is the result of two forces (Figure 1.11), Quadriceps force and Patellar tendon force, and has four functions [10]:

- Increases the lever arm of the quadriceps,
- Ensures stability under load,
- Allows the transmission of the quadriceps' force to the tibia,
- Provides bony protection to the trochlea and femoral condyles.

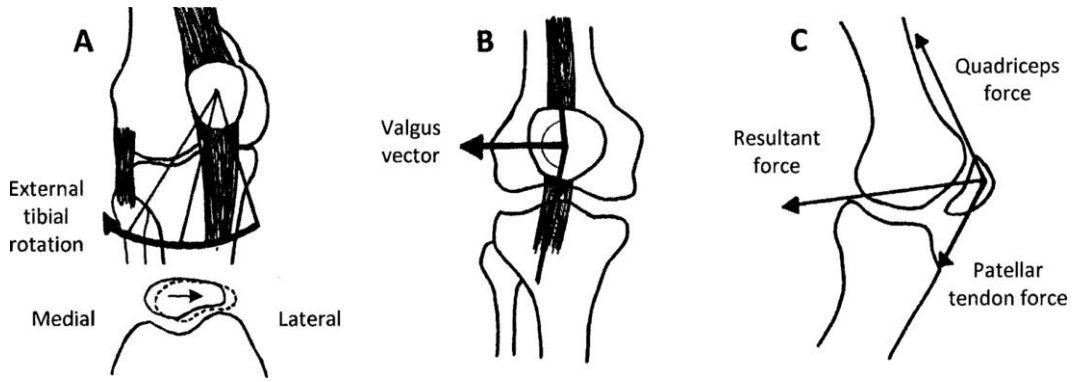

Figure 1.11: The patellofemoral joint.

This joint is characterized by a sliding movement: from full extension to full flexion, the patella slides over the femoral condyles. Additionally, since in a healthy human knee, the medial condyle is approximately 1.7 cm longer than the lateral condyle, the femur is not symmetric, but its axis is inclined by 3° relative to the central axis and 6° relative to the tibia. This is the reason why there is a resulting force from the patellofemoral joint that tends to push the patella laterally (the patella tends to lateralize) as shown in the Figure 1.11-A [13,14].

1.2. Problems requiring surgical intervention and the Knee Replacement

Comprehending the anatomy and biomechanics of joints holds significance in the realm of gait analysis, the identification of joint ailments, and the design and advancement of prosthetic implants. Joints possess a covering of hyaline cartilage, enabling the skeletal components to smoothly glide and rotate with minimal friction. Consequently, from a mechanical standpoint, joints endure substantial forces and moments, rendering them particularly prone to injuries. Notably, the primary cause of joint malfunction is linked to degenerative alterations in cartilage tissue, resulting in a reduction in the joint space and the convergence of the two bone ends. This diminishes joint stability, impairs mobility, and gives rise to painful and profoundly disabling symptoms [15].

1.2.1. Knee joint-related Pathologies

The causes of joint-related issues can be numerous, but they can essentially be attributed to two major categories: acute pathologies of traumatic origin and chronic overuse pathologies of degenerative nature. The primary knee pathologies that lead to degenerative and detrimental conditions for its structures encompass:

1. Osteoarthritis (OA): is an age-related cartilage disorder, usually occurring in people over 50 but also found in younger individuals. OA affects the entire joint and is the result of a complex

interplay of genetic, metabolic, biochemical, and biomechanical factors. it is due to wear and thinning of cartilage that causes bone structures to rub against each other [4,5]. If in a mild form, it does not lead to painful symptoms, and can be considered a normal consequence of ageing. While in a more severe form, damage to the articular cartilage, which in a healthy knee prevents pain (since it is not innervated), causes direct contact between the bone surfaces, increased vascularization, and pain. In its most severe manifestations (Figure 1.12), heightened cartilage degradation is linked to various factors, including the emergence of bony projections (osteophytes), which exacerbate mobility restrictions and induce discomfort. Additionally, there may be ligament laxity, weakening of the muscles surrounding the joint, thickening of the joint capsule, changes in the subchondral bone, and damage to the meniscus. These elements collectively result in an uneven distribution of forces, with the knee compartment bearing an disproportionately higher load, thereby accelerating the degeneration of the joint [19,20].

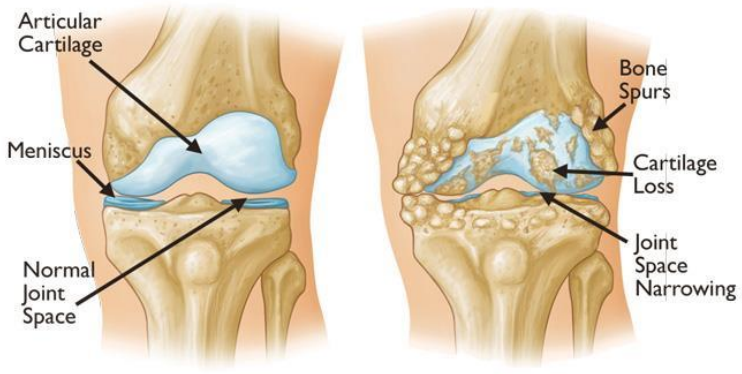

Figure 1.12: On the left side the healthy knee; on the right side the knee damaged due to OA.

2. Rheumatoid arthritis (RA): is an autoimmune disease that can occur at any age with a greater predisposition in women. it affects joint tissues as it causes the synovial membrane, which covers the joint capsule, to secrete inflammatory substances and attack the cartilage, leading to the deterioration of the latter, but also of other structures and sometimes organs.

3. Post-traumatic arthritis represents a significant concern among young and physically active individuals, arising from cartilage damage that develops gradually as a result of bone fractures or tears in tendons or ligaments. This condition results in pain and restricted joint functionality [4].
4. Avascular necrosis (AVN) occurs when bone cells die due to inadequate blood supply within the joint, leading to the loss of articular cartilage. This condition puts bones at risk of collapsing, resulting in pain and loss of joint function.

Finally, less common occurrences and less serious may include injuries like meniscal injuries, tendonitis, fractures, cartilage injuries, patellar syndromes, and ligamentous injuries. These risks may be heightened by factors such as obesity, gender, and age.

1.2.2. Total Knee Arthroplasty

Prosthetic therapy is often the optimal choice in cases of severe osteoarthritis, joint instability, as well as conditions involving tumors and post-traumatic injuries. This approach is specifically designed to alleviate pain and restore full joint functionality. Joint arthroplasty or replacement surgery is the core of this treatment, involving the replacement of the arthritic or dysfunctional joint surface with an orthopedic prosthesis or implant. This surgical procedure within the field of orthopedics focuses on replacing, modifying, or repositioning the joint surface in musculoskeletal joints, employing techniques like osteotomy and other surgical interventions [21].

Hence, knee joint replacement surgery is conducted when a clinical examination reveals a painful restriction of movement accompanied by joint cracking, as well as the presence of redness and warmth.

Total Knee Arthroplasty (TKA) is regarded as the primary treatment for advanced knee osteoarthritis (OA) and is equally applicable for various other underlying conditions, such as inflammatory arthritis, fractures (potentially leading to post-traumatic OA or deformity), dysplasia, and malignancy [3]. TKA stands out as one of the most successful and cost-effective interventions in the orthopedic field, boasting a five-decade history of using this prosthesis to address chronic degenerative knee conditions.

Presently, there is a notable global surge in the demand for TKA, driven by the increasing prevalence of knee arthritis. Projections indicate an 85% growth in the number of primary TKA procedures (reaching 1.26 million procedures) by 2030.

1.2.2.1. TKA designs

Throughout these five decades, the partnership between surgeons and engineers has resulted in numerous innovations in TKA design, and we can confidently state that at present, this procedure is secure and firmly established [70,71,73].

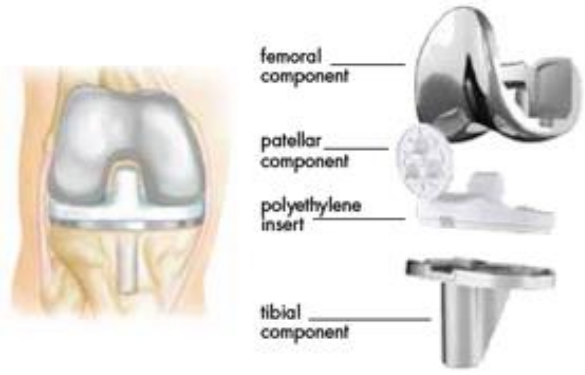

Figure 1.13: The TKA components.

The knee prosthesis comprises three main components (as shown in Figure 1.13):

1. The femoral component: It replaces the distal part of the femur. In many cases, the implant is designed asymmetrically to better mimic the asymmetrical geometry of the native femoral

condyles. Modern designs feature a smooth deep groove with a short, narrow notch, improving patellar tracking and stability to prevent potential patella dislocation. It is typically constructed from strong polished metal, with Cobalt-Chrome (CoCr) being a common material choice [4].

2. The tibial insert: This component fills the gap between the distal femur and the proximal tibia, which results from the removal of the menisci. The insert plays a vital role as a shock absorber, facilitating smooth gliding, absorbing shocks, and preventing dislocation. Ultra-High Molecular Weight Polyethylene (UHMWPE) is the usual material used for the insert, known for its excellent mechanical properties, including impact resistance, abrasion resistance, strength, fatigue resistance, elasticity, low friction coefficients, chemical inertness, and biocompatibility [22].
3. The tibial component: It consists of a flat plate and a short stabilizer stem inserted into the central part of the tibial bone. The tibial component is typically composed of metal, commonly Cobalt-Chrome or a Titanium alloy.

Furthermore, some researchers advocate for resurfacing the patella during knee arthroplasty, while many surgeons prefer to implant the patellar component only in specific cases. The patellar component is made of UHMWPE and is always cemented in place [4].

For many patients, undergoing Total Knee Arthroplasty (TKA) enables a return to basic activities like walking and climbing stairs, significantly enhancing their quality of life by reducing pain and improving mobility. The market offers a variety of TKA designs tailored to different knee joint conditions, aiming to meet individual patient requirements.

Nevertheless, orthopedic surgeons and patients alike are striving for enhanced functional outcomes. Hence, the collaboration between engineers and orthopedic surgeons plays a pivotal role in evaluating and enhancing existing prosthetic designs or potentially creating new ones. With

advancements in technology and the utilization of innovative materials, traditional techniques have been reexamined to improve their effectiveness. Each design concept focuses on specific aspects such as maximizing range of motion (ROM), minimizing pain and debris, optimizing joint geometry, selecting appropriate fixation methods, improving component and stem modularity, determining constraint types, evaluating knee kinematics, and managing costs [23].

Knee prostheses can be classified based on different criteria.

A classification of knee prostheses can be conducted based **on the mechanical constraint present and the condition of the posterior cruciate ligament** (Figure 1.14) [12,18,26,27]:

- Cruciate Retaining TKA (CR TKA), a covering (unbound) prosthesis with preservation of the posterior cruciate ligament,
- Posterior-Stabilized TKA (PS TKA), a semi-bound prosthesis in which the cruciate is sacrificed,
- Constrained-Condylar fixed-bearing TKA (CCK TKA), in which the medial compartment determines the stability of the knee,
- Hinged TKA (bonded).

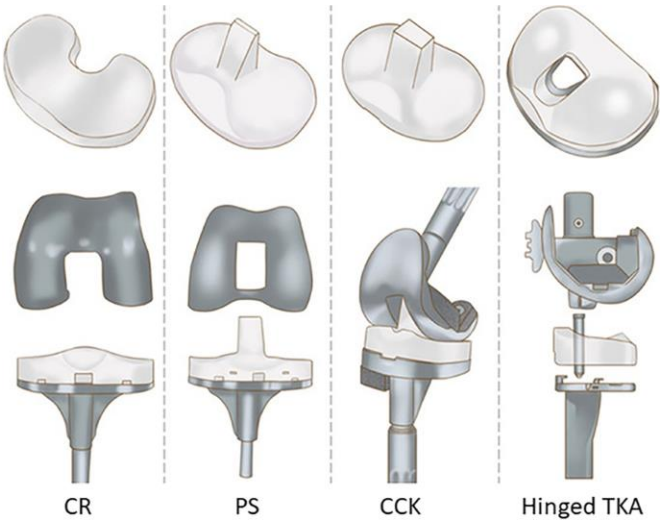

Figure 1.14: Classification of knee prostheses based on the mechanical constraint present and the condition of the posterior cruciate ligament.

Another classification is based on the **type of fixation used**:

- Cemented prosthesis (the femoral component is generally fixed to the bone using acrylic cement),
- Non-cemented prosthesis (cementless porous components are mainly used in the tibial component),
- Hybrid prosthesis (cemented and cementless),

Furthermore, according to the meniscal component chosen, i.e. according to **the mobility of the polyethylene pad interposed between the tibia and femur**, we can have:

- Prosthesis with fixed PE (polyethylene) insert,
- Prosthesis with a mobile PE insert. This type of prosthesis simulates the behavior of the menisci with the aim of creating an element that simulates a bearing that can move in the tibial plane. The main advantage is a greater contact surface between the femur and PE in all knee configurations. The disadvantage is that the bearing wears out due to possible wear on the upper and lower bearing surface and delamination phenomena due to shear actions [24,25,28,68].

Finally, it's important to focus on the type of knee prosthesis that can be created, because knee prostheses can be classified based on the **replaced compartments** [16,17]:

- Unicompartmental prostheses,
- Bicompartmental prostheses,
- Tricompartmental prostheses without an artificial patella,
- Tricompartmental prostheses with an artificial patella.

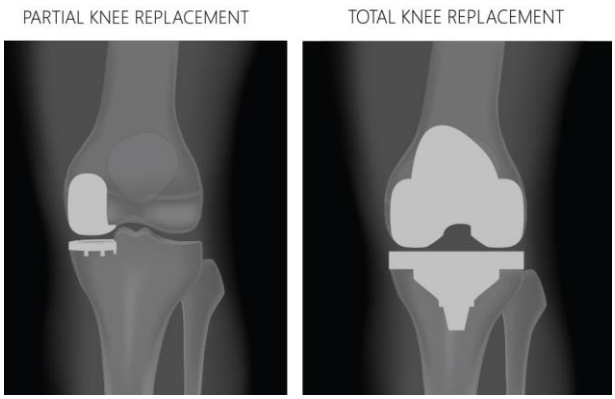

Figure 1.15: On the left side the UKA; on the right side the TKA.

Therefore, it is possible to completely replace the knee joint with a total knee arthroplasty (TKA) or, in some cases, address the issue with a unicompartmental knee arthroplasty (UKA), which involves less invasiveness and shorter recovery times (Figure 1.15). Indeed, UKA seems to offer advantages in terms of functional recovery, especially by preserving joint structures. However, there are disadvantages associated with this procedure, such as the potential deterioration of non-prosthetic parts, the need for surgical precision, and the risk of sinking or more frequent mobilization due to long-term shear stresses. In cases where cartilage wear affects all joint components, the implantation of a total prosthesis becomes necessary, a procedure that involves a significant sacrifice of bone and cruciate ligaments.

1.2.2.2. Revision TKA

As previously mentioned in the preceding paragraph, innovations in this field range from traditional covering prostheses to constrained and meniscal-bearing prostheses. Furthermore, orthopedic surgery has witnessed the introduction of various technology-assisted techniques, such as robots, patient-specific cutting guides, preoperative software, and computer-assisted navigation systems. These innovations have significantly improved accuracy and reproducibility in maintaining bone resections and ligament balance. However, other issues related to total knee arthroplasty (TKA),

such as prosthesis survival, revision surgery, as well as the management of post-operative complications and rehabilitation, are significant topics that deserve further exploration.

When delving into the specific factors contributing to TKA failures, it proves highly advantageous to differentiate between early and late failures. Early failure necessitates revision surgery within the initial two years following the procedure [72]. In instances of early failure, patients frequently encounter issues right from the outset, manifesting a range of symptoms such as pain, swelling, instability, and limited range of motion. The underlying causes of early failure typically originate from the surgical process itself, encompassing factors like infection, improper positioning, instability, and complications related to the patellofemoral joint. In contrast, late failures are more likely attributable to problems associated with the implant, including aseptic loosening, persistent instability, and recurrent infections.

Significantly, scientific studies in the medical literature have underscored that one of the most severe complications arising after total knee arthroplasty (TKA) is periprosthetic joint infection (PJI) [67]. Despite substantial progress in the realms of prevention, diagnosis, and treatment of PJI, it remains the most commonly reported cause of early TKA failure, ultimately necessitating revision surgeries. Regardless of the situation, it is crucial to create a pre-operative diagnostic algorithm that can accurately identify the cause of failure. This is particularly important due to the extensive list of failure modes, as it helps prevent the recurrence of the same error and sets the stage, alongside other factors, for the revision surgery.

In contrast to primary TKA, performing R-TKA (revision TKA) presents significantly greater surgical challenges, demanding more advanced techniques to achieve a secure implant fixation and establish a well-balanced knee with equal spaces in both extension and flexion.

The primary objective of the reimplantation procedure is to eliminate the infection and restore a functional and stable joint while reducing pain. Typically, addressing PJI requires more than just

antibiotics; it involves surgical interventions like irrigation and debridement, two-stage reimplantation, one-stage reimplantation, resection arthroplasty, or even amputation in some cases [69].

Because of a range of factors, there has been a notable uptick in TKA revisions in recent years, and this trend is expected to continue. A key driver behind this increase is the rising number of primary TKAs. Additionally, younger patients are now undergoing TKA procedures due to favorable outcomes, greater activity expectations, and increased acceptance of the surgery. Moreover, obesity, particularly in the Western world, plays a significant role in this trend. In summary, the projected increase in TKA revisions in the United States far exceeds the growth rate of primary TKAs [71,73].

Hence the need to also analyze the problems that the revisions of TKA may encounter and to find innovative solutions that can avoid drastic decisions such as amputation.

The next chapter will explore this topic in more detail.

Chapter 2

State of the art

2.1. Clinical Context

Continuing with the topic treated in the previous chapter, within the context of Revision Total Knee Arthroplasty (R-TKA), infection remains the primary cause of failure [75]. The other two prevalent factors are loosening of the tibiofemoral implant and wear of the polyethylene component. These problems result from inadequate long-term fixation and, additionally, a high level of constraint [69].

It is important to emphasize once again that in the case of R-TKA, prosthesis stability is crucial. However, in patients who have undergone multiple revisions, or severe post-implant or post-traumatic infections, or have a tumor, it is common to find extremely weak, fragile bones with significant defects, making it extremely challenging to achieve good fixation and adequate prosthesis stability [72].

This study specifically addresses this range of patients who, until a few years ago, had amputation as their only solution [74]. The need is to develop implants able of adapt to the patient's bone morphology, replacing bone defects and promoting osseointegration.

2.2. Technological Context

Before illustrating the innovations that R-TKA has undergone in recent years, it is necessary and essential to focus on the technologies used in the fabrication of prosthetic components.

Additive Manufacturing, or AM, is an industrial process used to manufacture objects from 3D computer models by adding one layer on top of another, as opposed to traditional subtractive manufacturing methods (milling machines or lathes), which start with a block of material from which chips are mechanically removed.

In detail, the Powder-Based Electron Beam Additive Manufacturing Technology (EBAM) is a relatively new additive manufacturing (AM) process that can produce fully dense metal parts directly from electronic data of the designed part's geometry using powders [80].

Specifically, The Powder Manufacturing technology involves that the CAD model is “sliced” by a special software in sections 50 microns thick. Each section is stored in the Computer Memory. Thereafter, production is ready to start in the machine working area. The entire process is performed at high temperature in a vacuum environment. The electron Beam “draws” the section and powder melts when touched by it. Once a section is completed another layer of powder is added and the process re-starts. After the cooling down the working area is open and the powder mass with the implants inside is taken out. When the powder in excess is removed using compressed air, implants appear inside the powder mass and are collected and sent to polishing. Finally, polishing, and final finishing is then made employing standard techniques [78].

EBAM has gained significant attention from various sectors, including the biomedical field and orthopedic applications, with appropriate materials [82,83,84].

Titanium alloy (Ti-6Al-4V) has been shown to be one of the most widely used materials in orthopedics, because titanium, among implant materials, has the lowest elastic modulus, making it closer to that of cortical bone. This allows for a much more effective distribution of load between bone and implant compared to other alloys. In the post-implantation phase, we have a situation where the two elements, both capable of elastic deformation, must communicate with each other, meaning that the metal must osseointegrate. This is achieved when the metal's stiffness is as low as possible, allowing bone to remodel itself in a physiological and healthy way and avoiding the problem of stress shielding (where the bone tends to resorb). Furthermore, titanium alloys (Ti-6Al-4V) also exhibit other properties such as high mechanical strength, high corrosion resistance, and good biocompatibility. The latter is essential to prevent post-surgical infections [82-85].

Normally, Titanium is used for tibial implants and femoral and tibial cementless stems or cementless tibial base prostheses because the adhesion of cement to titanium is not optimal, and it is not used for femoral components due to its insufficient wear resistance [82].

Since 2007, Adler Ortho company has been gradually incorporating Powder Manufacturing Technology into the manufacturing process of Hip, Knee, limb salvage prostheses, Trauma devices, surgical instruments, and Custom implants, using Titanium, Stainless Steel, and CoCrMo alloys, thus succeeding in transforming what used to be a prototyping process into a very powerful system for the industrial production of joint prostheses [78].

Aware of the advantage that powder technology and the use of titanium alloys could provide, the research of the Adler Ortho team led to the development of **cementless tibial base prostheses in titanium alloys with a monolithic three-dimensional Ti-Por (porous or trabecular titanium) surface** (Figure 2.1) [77].

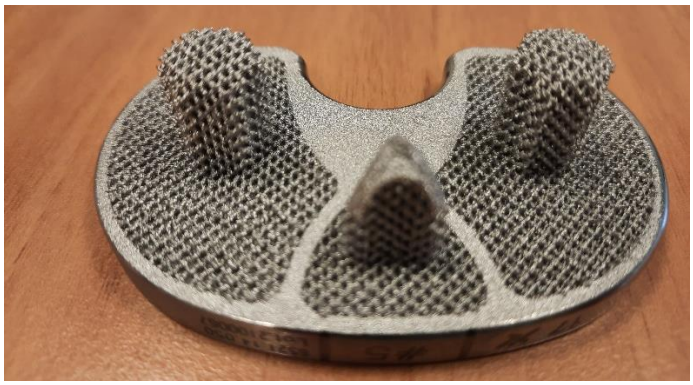

Figure 2.1: Cementless tibial base prothesis in titanium alloys realized with EBAM.

The surface of these prostheses appears to be coated with porous titanium, with mechanical characteristics compatible with those of the spongy bone tissue, which is also a porous material, and appears extremely rough and durable (Figure 2.2), ideal for maximizing the primary stability of prostheses and subsequent integration by the host bone [77].

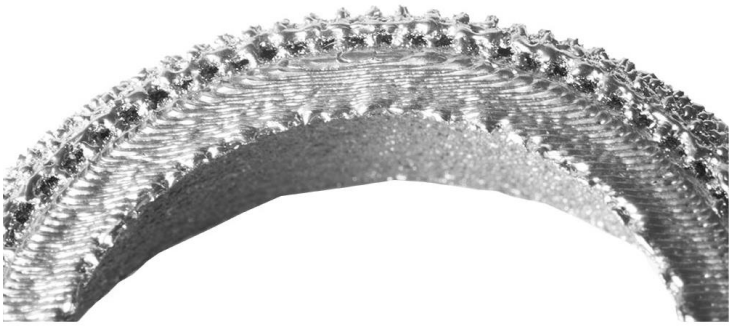

Figure 2.2: Section and enlargement of the Ti-Por surface.

As already mentioned, when using powder technology, prosthetic components are created directly from metal powders without the use of any physical instruments [78]. The implant is produced layer by layer, and at the end of the process, it is basically complete as can be shown in Figure 2.3:

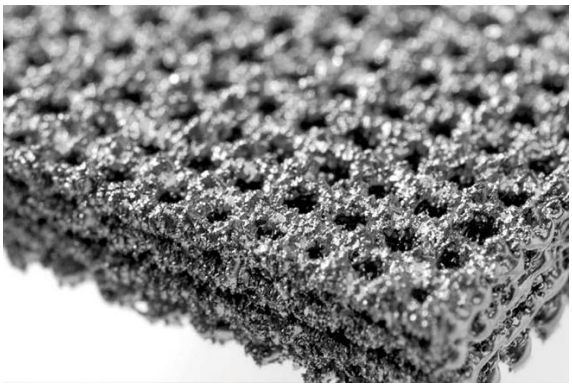

Figure 2.3: Creation of the one-piece structure layer by layer using powder technology.

In this way, it is possible to design and produce relatively easily and quickly even very complex custom-made implants for oncological applications or for the revision of joint implants where there is a massive bone lack. The custom-made implants thus produced are patient-specific because they are able to fit the patient's bone defect perfectly. These structures have a morphology very similar to the trabecular structure of cancellous bone, the only difference being that the trabeculae have formed through a technique and not intelligently as in bone. The shape and size of interconnected pores ensure bone growth and proper vascularization in all of its parts [79,82-85]. An example of a patient-specific reproduction of a hip prosthesis made using powder technology is shown in Figure 2.4:

Figure 2.4: Patient-specific reproduction of a hip prosthesis made using powder technology.

To obtain 3D computer models required for printing in Ti-Por, it begins with a tomographic analysis or magnetic resonance analysis of the patient's bone structure that needs to be recreated. Then, DICOM files are converted into a CAD design (computer model), which is then transferred to additive manufacturing or rapid prototyping equipment and the result is that the real biological structure of the patient's bone is recreated layer by layer by this additive manufacturing technique [64-66,81].

Finally, another important aspect is that titanium can be 3D-printed by modulating the porosity and consequent biomechanical properties to best mimic bone.

2.3. Purpose

The clinical need for custom-made implants, coupled with innovative powder technology, has led to the development of porous custom-made cones for the reconstruction of meta-diaphyseal bone defects in knee revision surgery [51,60]. This study involves a real clinical case in which a patient, with severely compromised bone conditions after numerous revisions, received custom-made porous titanium cones along the tibial and femoral diaphysis.

To evaluate the actual benefits brought about by the use of patient-specific ADLER cones, a biomechanical analysis was conducted. This analysis, based on previously validated finite element models, examines and compares stress distribution on both the tibia and femur resulting from cone utilization versus traditional fixation techniques using cemented and press-fit prosthetic stems. Furthermore, the advantage of using porous titanium (Ti-Por) over solid titanium (conventional) was analyzed. This is a static analysis that assesses daily activities such as full extension (at 0°) and chair-rise (at 90°).

The aim of the biomechanical analysis is to examine whether custom-made cones can restore the patient's ability to perform simple daily activities compared to traditional revision implants and demonstrate that they provide a good bone-prosthesis interface with limited stress peaks and even stress distribution along the entire bone.

Chapter 3

Finite Element Analysis

3.1. What's Finite Element Analysis?

The morphology of bone is primarily determined by genetic factors because, when analyzing bone, there are no precisely defined angles, curves, and distances, but rather a patient-specific morphology that is highly heterogeneous and changes throughout life, depending on physiological loads, health, age, and nutrition. However, it is also influenced by mechanics, as bone has the ability to adapt to mechanical loads. This means that the external and internal structure of bone transforms in response to the loads acting upon it, as stated by Wolff's law in 1892 [86].

It is easy to understand how this bone transformation plays a crucial role in implant technology and arthroplasty. If, during surgery, the biomechanical distribution of forces in and around the treated joint is reconstructed inappropriately or if the implant design is inadequate, the result can lead to a situation where the primary forces are mainly transferred by the implant, while adjacent bone regions receive minimal loading and may undergo degeneration (stress shielding) [87].

This problem can be addressed and prevented through an analysis of the stresses and deformations in the composite formed by the implant and bone.

To develop a stress and deformation analysis of the bone structure with or without prosthesis integration, it is appropriate to first construct the finite element model using the Finite Element Structural Analysis Method (FEM) and then to proceed with Finite Element Analysis (FEA) [61-63,76]. The latter is a numerical method used to analyze, compare, and predict the behavior of a part or

assembly under certain conditions. It is used as the basis for modern simulation software and helps engineers find weak points, areas of tension, etc. in their designs.

Figure 3.1 illustrates the necessary and indispensable steps that precede FEA. Firstly, CT images are obtained by means of preoperative computed tomography. Using appropriate software, the raw tomography data (DICOM files) are transformed into files ready for the construction of the contour lines and the surface of the bone of which the model is to be built [65,66]. Thus, one goes from information on many images to an image that mathematically defines the contours and surfaces of the structure to be built, using image segmentation techniques. The three-dimensional model of the bone structure is thus obtained, ready to be exported to a CAD (Computer Aided Design) or FEM environment [81].

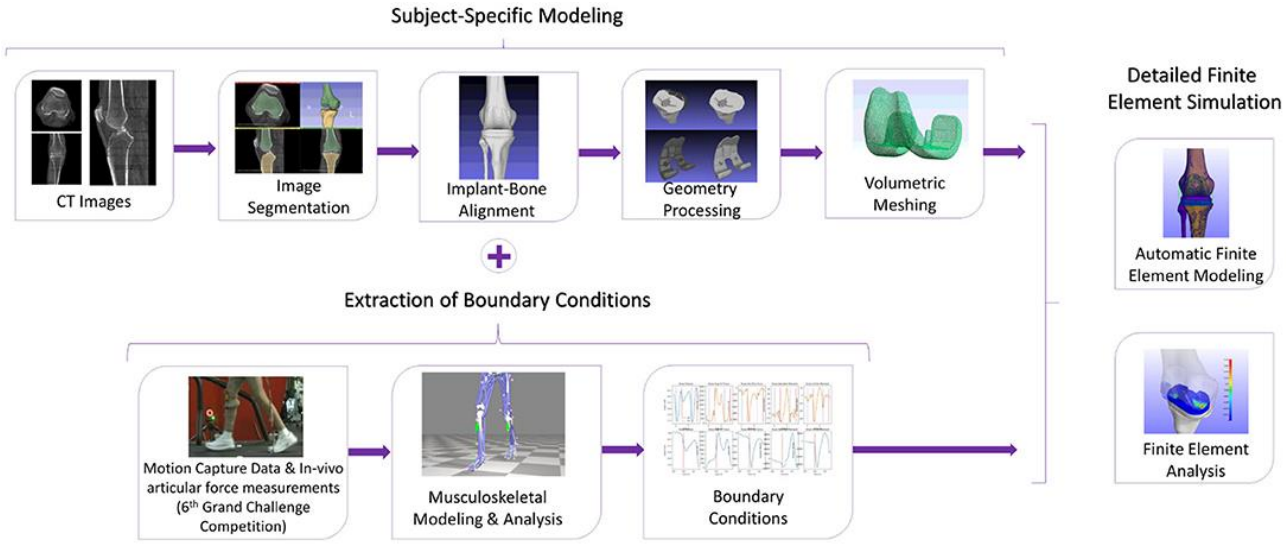

Figure 3.1: All steps required to perform the FEA from CT images [62].

With CAD software, one goes from creating surfaces to creating volumes, achieving the correct implant-bone alignment when necessary. This is because CAD/CAM (Computer-Aided Design/Computer-Aided Manufacturing) technology is characterized by excellent accuracy in positioning the prosthetic implant with simplified operations [64,81].

However, to analyze the behavior of the 3D object under the action of certain loads, CAE tools are used. Computer-aided engineering (CAE) is a rapidly expanding field that takes CAD to another level. While CAD is useful for creating 2D and 3D models of a product, CAE software allows for a more detailed engineering analysis of objects and encompasses not only CAD, but also computer-aided manufacturing (CAM), finite element analysis (FEA), computational fluid dynamics (CFD) and some other aspects of engineering.

Then, once the CAD models of the implants and bones have been obtained, they can be directly imported into more advanced software. They start with a pre-processing phase, in which the model is 'prepared' by modifying the geometry, applying boundary conditions, defining material properties and part interactions, and creating the finite element (FE) model through the mesh. After the geometry has been discretized from the continuum with finite elements (mesh), the outputs to be visualized are requested and the simulation (FEA) is executed [61-63,76].

For this study, a finite element analysis was performed using ABAQUS/Explicit version 2019 (Dassault Systèmes, Vélizy- Villacoublay, France) software.

3.2. ABAQUS Steps

This section will specifically explain all the steps implemented in the ABAQUS software.

3.2.1. Geometry

For the biomechanical analysis, firstly, CAD models of the patient's bones (femur and tibia), realized by Adler Ortho's team, were imported, which were already positioned in the xyz plane with their correct anatomical orientation.

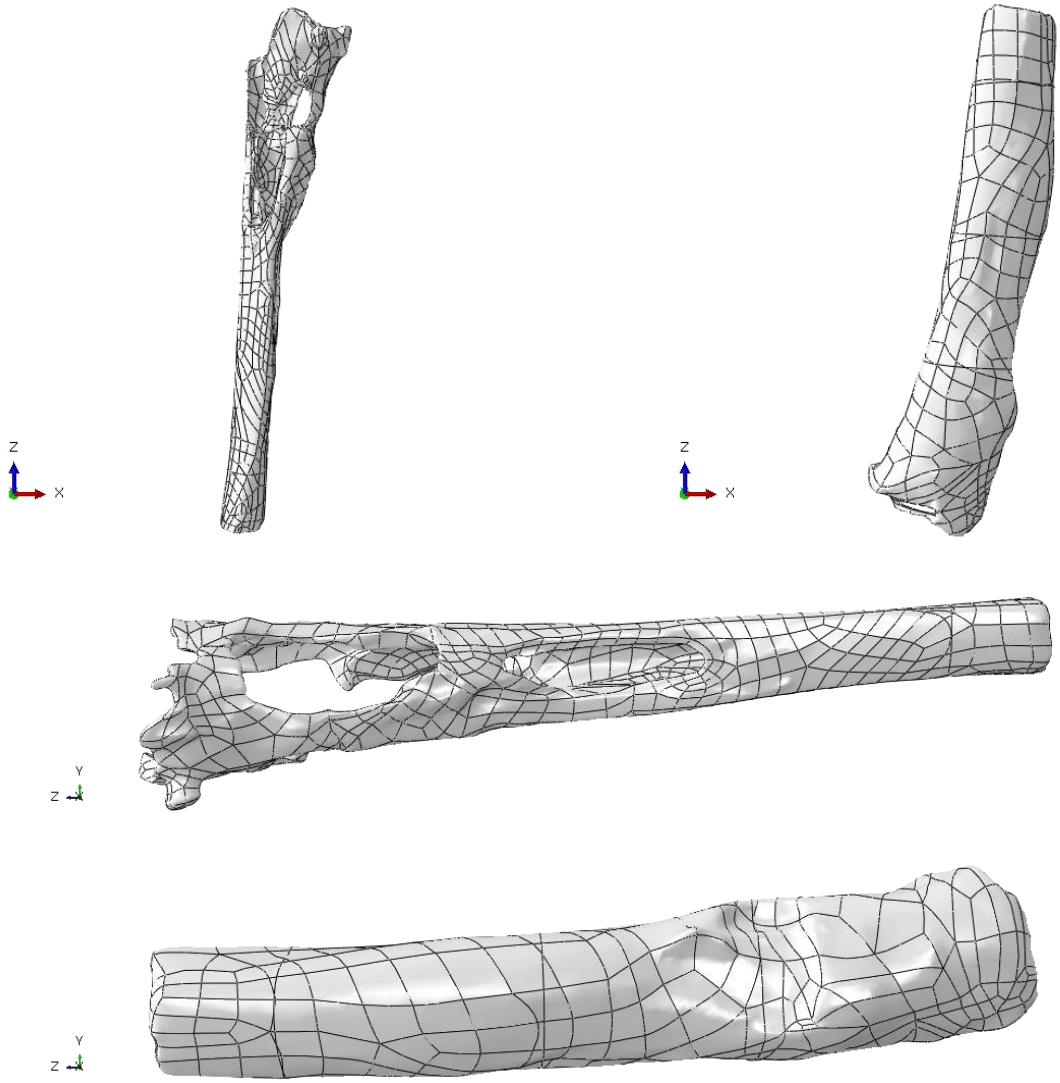

Figure 3.2: Bone morphology of patient's tibia and femur from different points of view.

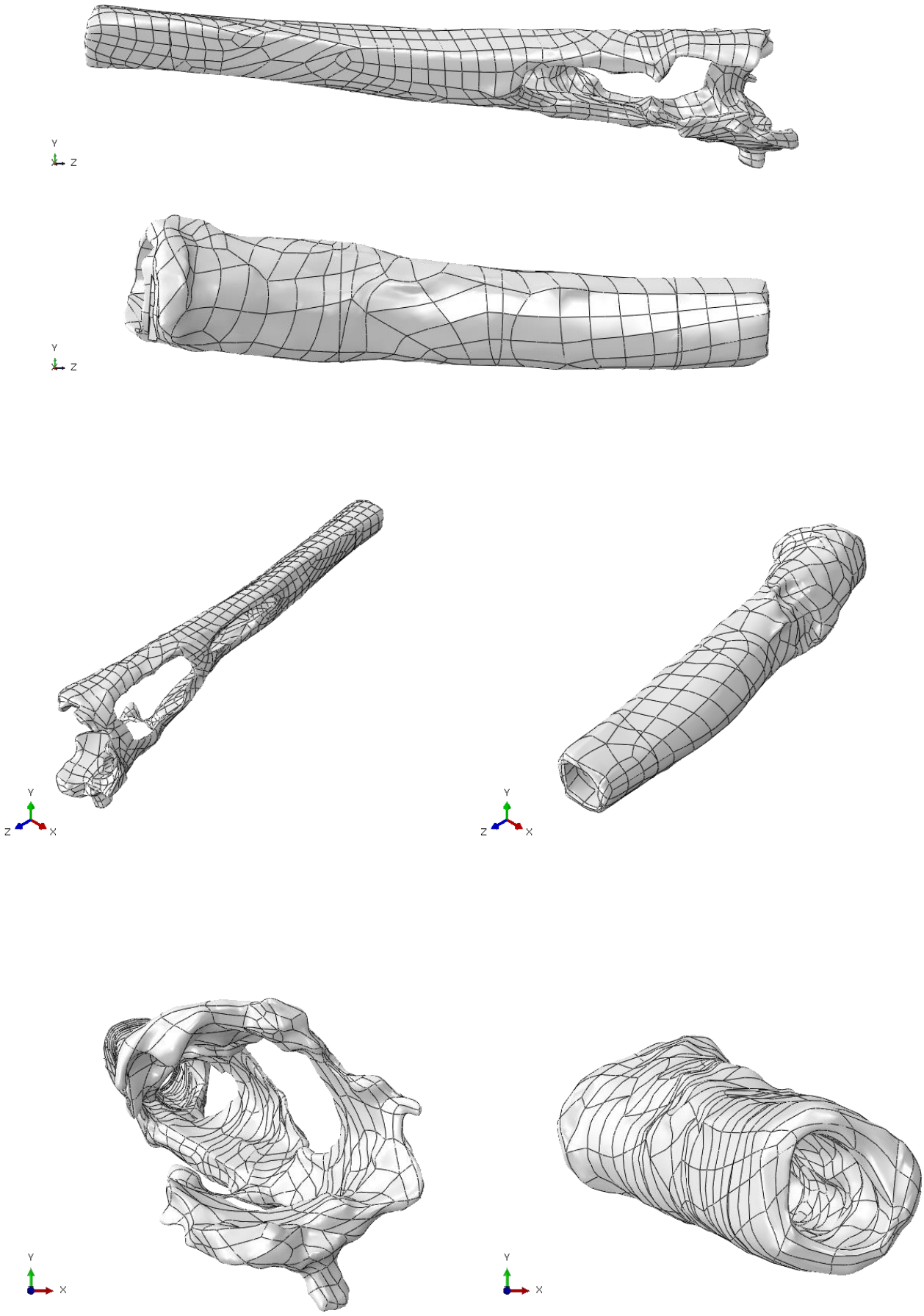

Figure 3.2: Bone morphology of patient's tibia and femur from different points of view.

As is evident from all Figures 3.2, the tibia and femur of the left leg are completely compromised, especially in the area proximal to the implant, which is missing the medial and lateral epicondyles and condyles, and the tibial plateau. The cortical bones have large holes that show the lack of the cancellous part of both the femoral and tibial bones. To replace the task performed by the cancellous bone, a solid with the properties of orthopedic implant cement will be inserted later to fix the bone to implant.

The mechanical axis of the knee joins the centre of rotation of the femoral head with the intercondylar fossa and is coincident for both femur and tibia. While the anatomical axis coincides with the diaphyseal axis of the bone itself, it will be different for the femur because it is displaced by an angle Q (Figure 3.3) with respect to the mechanical axis [88].

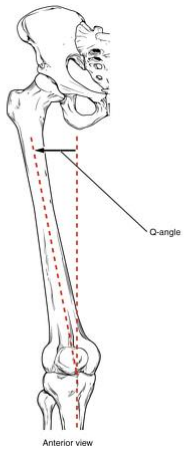

Figure 3.3: Q angle in the femur.

This difference can be seen in Figure 3.4, in which the mechanical axis of the knee and the anatomical axis of the femur are represented:

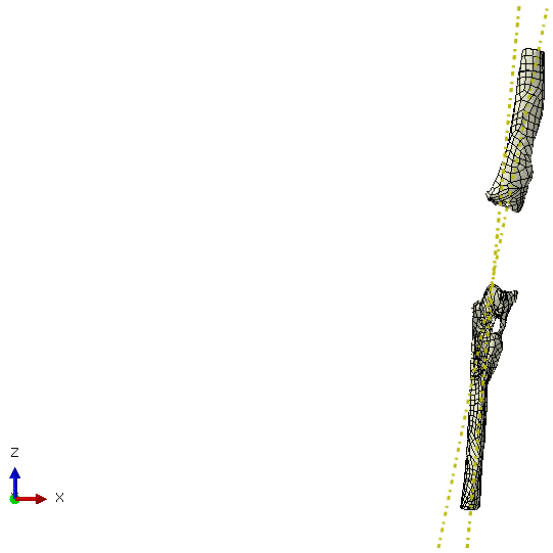

Figure 3.4: Difference between mechanical and anatomical axis.

To these tibia and femur files were adapted the five CAD models of the prosthetic implants, also supplied to me by Adler Ortho, whose geometries will be explained in the following subsections.

3.2.1.1. First Model: R-TKA with porous titanium cones

The first model is the hinged revision prosthesis from the company Adler Ortho, called 'Genus Pantheon', combined with custom-made cones.

These cones are called bimaterials because they have a titanium alloy skeleton and a porous titanium core. Porous titanium cones are created using Powder Manufacturing technology and are identified with the Tri-Por® symbol, a registered trademark of Adler Ortho. The porosity of porous titanium is 58%, which means it weighs 0.42 compared to pure titanium. The geometry of the cones is the same for the femur and tibia and in both cases extends from the proximal part of the bone along the entire diaphysis of the bone. Between the cone and the bone, and between the cone and stem, orthopedic bone cement (made of PMMA) was inserted, which makes bone-cone and cone-prosthesis adhesion possible, in the absence of the cancellous bone. The bone cement was created through the use of Boolean subtraction, which subtracts 3D objects from another 3D object and a

new object is created. Initially, a rectangular parallelepiped was created that was large enough to hold the bones inside. Then, with an initial Boolean operation, the tibia and femur were subtracted from the created solid, resulting in the internal bone filler inside the parallelepiped. Following the removal of the excess parts, a second Boolean subtraction was performed between the inner filler of the femur and tibia with the femoral and tibial cone respectively. In this way, both the cement between cone and bone and the cement between cone and stem were obtained for the femur and tibia.

Figure 3.5-a shows the assembly of the hinged prosthesis consisting of: femoral component (in green); tibial insert (in red); additional inserts that provide stability for the tibial plateau, which is difficult to insert in other ways (in grey); tibial component (in light grey); femoral and tibial stem (in blue). Figure 3.5-b shows the addition of cement between stem and cone (in yellow), Figure 3.5-c that of the tibial and femoral cones (in orange), Figure 3.5-d that of cement between cone and bone (in yellow) and finally Figure 3.5-e the bones are added.

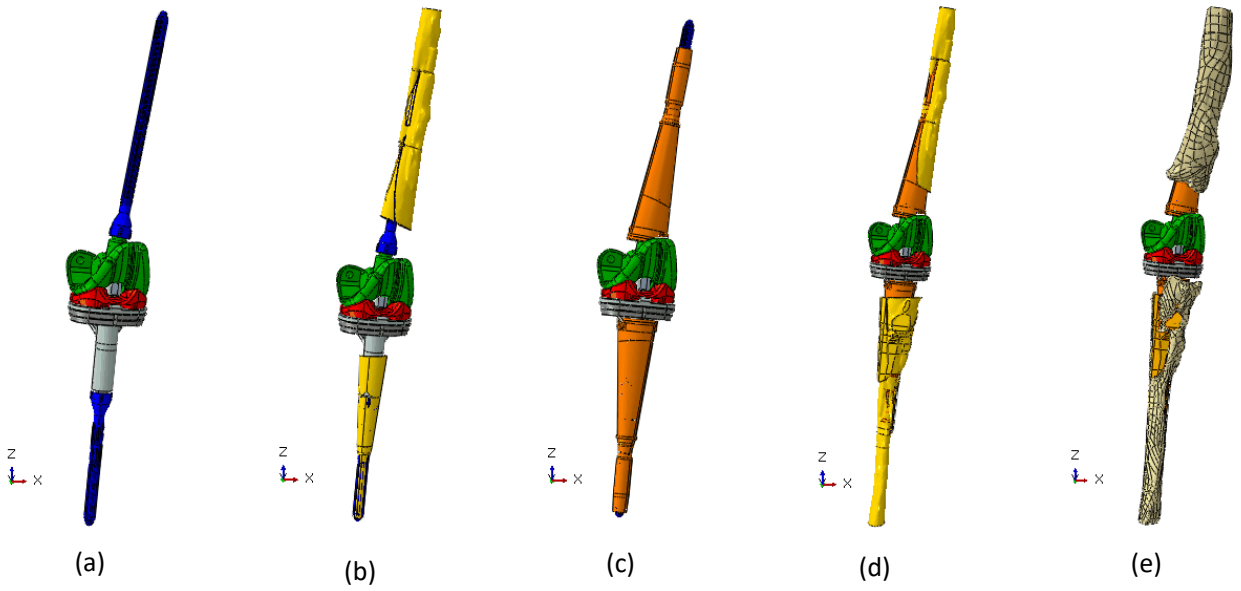

Figure 3.5: Assembly of the first model step by step starting with the hinge prosthesis (a), with the addition of cement interposed between stems and cones (b), with the addition of cones (c), with the addition of cement interposed between cones and bones (d).

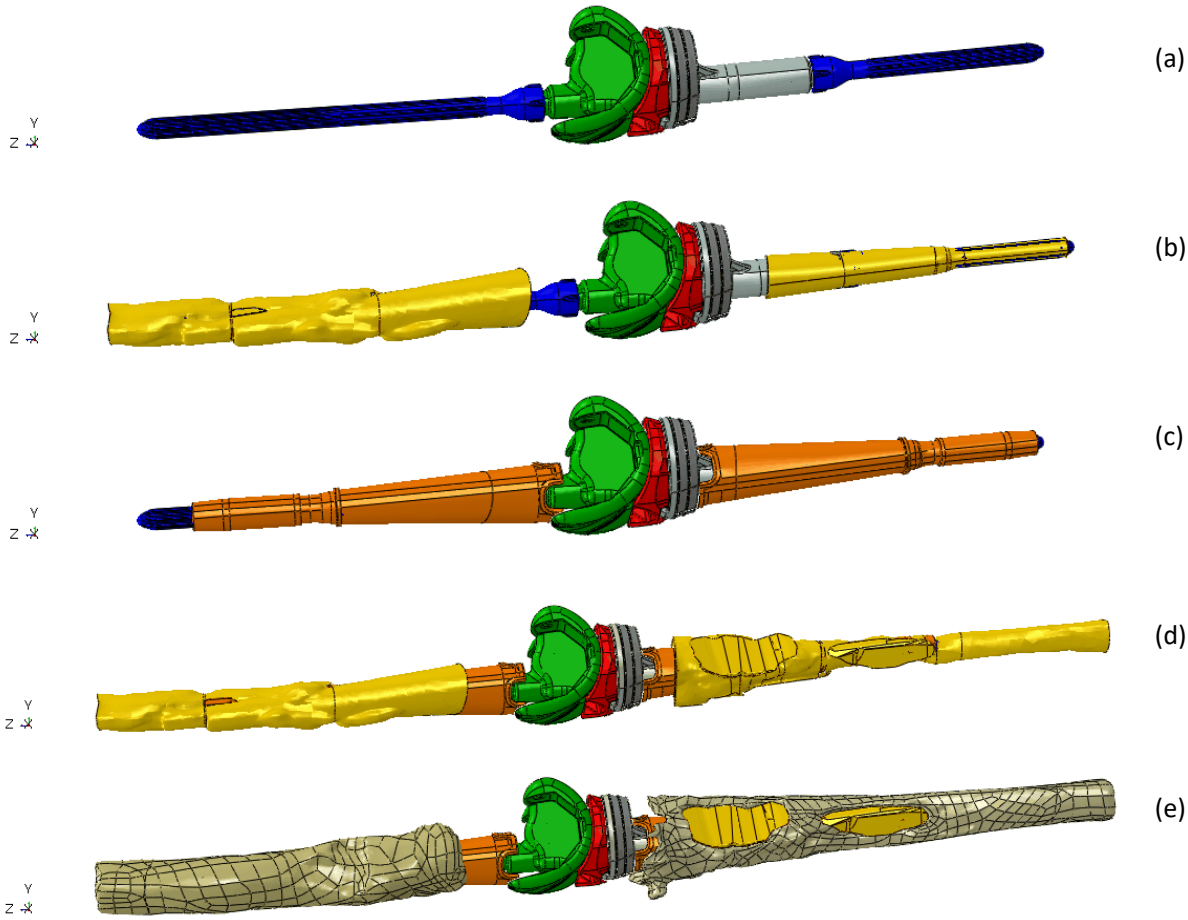

Figure 3.6: Assembly of the first model step by step, laterally, starting with the hinge prosthesis (a), with the addition of cement interposed between stems and cones (b), with the addition of cones (c), with the addition of cement interposed between cones and bones (d).

The entire assembly of the first model is shown, with a side view, in Figure 3.6 (a) - (e).

As regards the hinged prosthesis, given the lack of an anatomical centre of rotation of the knee, it was constructed to impose a mechanical centre of rotation by adding specific components built specifically for this clinical case. these are shown in Figure 3.7 in different colours according to the material from which they are made. there are components in CoCrMo alloys (in green), in titanium alloys (in grey) and in HMWPE (in bronze). To give the reader a better understanding of the additional components produced by Adler Ortho, they are shown in front view in Figure 3.8-a, side view in Figure 3.8-b and rear view in Figure 3.8-c. While an overview of these, with femoral and tibial component and insert, is shown in Figure 3.9, from an anterior (a), posterior (b), lateral (c) and medial (d) viewpoint.

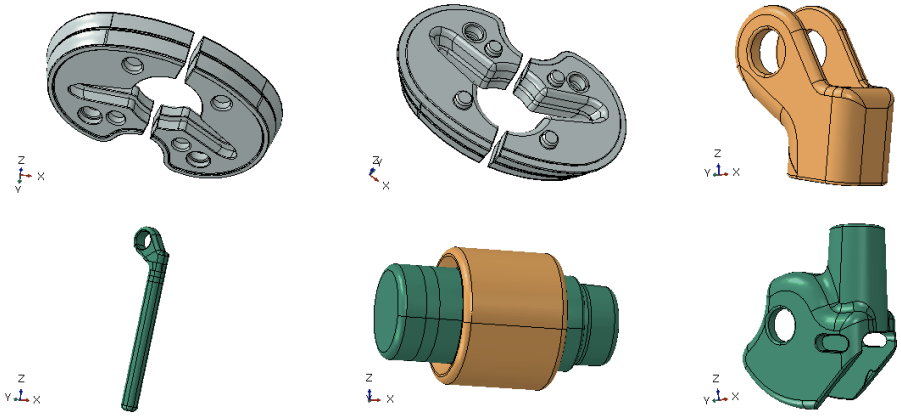

Figure 3.7: Additional components in R-TKA hinge used for all 5 models.

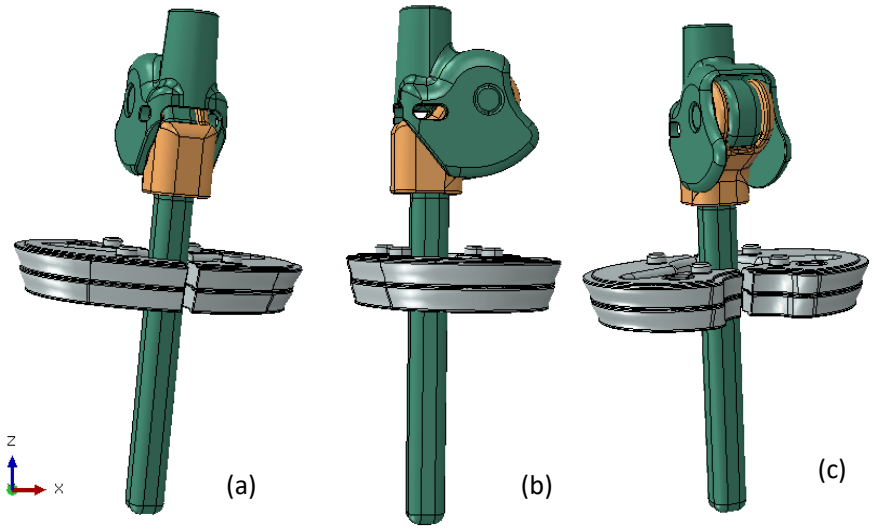

Figure 3.8: Assembly of additional components in R-TKA hinge used for all 5 models, in anterior (a), lateral (b), and posterior view (c).

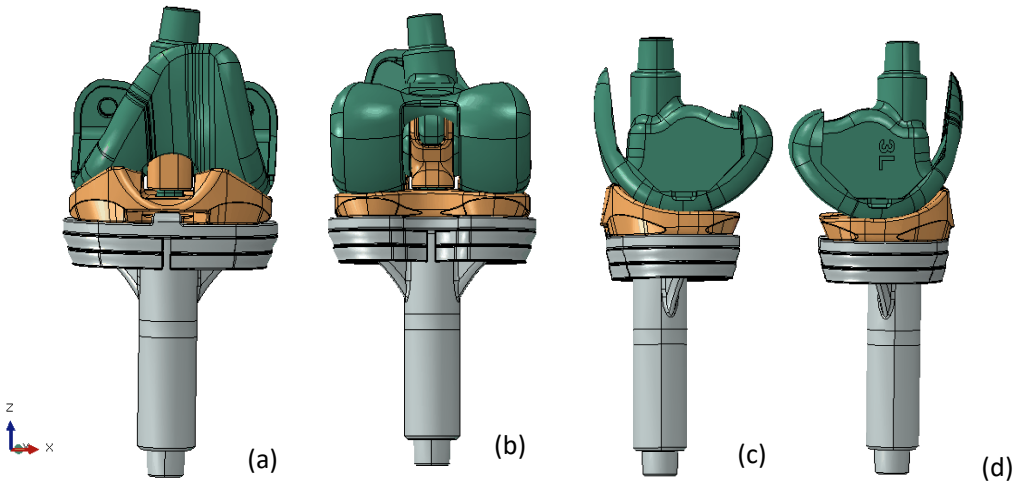

Figure 3.9: Assembly of total hinged R-TKA used for all 5 models, in anterior (a), posterior (b), lateral (c), and medial view (d).

3.2.1.2. Second Model: R-TKA with solid titanium cones

The second model is identical to the first model, a 'Genus Pantheon' hinged revision TKA combined with the cones, with the exception of the femoral and tibial cones in terms of materials and geometry. The cones of second model are entirely in porous titanium but with a different porosity, i.e. they are "full" cones (conventional, based on previous literature works) with porosity close to 0% and with a weight equal to that of pure titanium. While the geometry of the solid cone (Figure 3.10) is not very different from that of the bimaterial cone (Figure 3.11). The properties of the materials will be explained and deepened in the “Materials and Property” section.

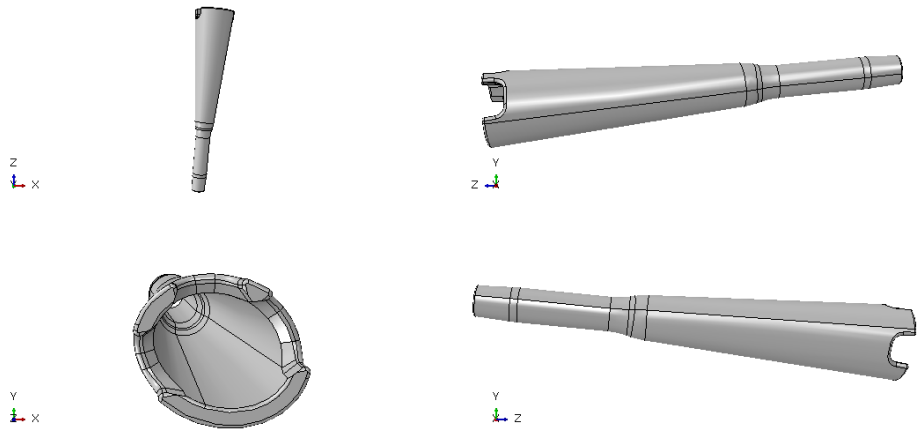

Figure 3.10: Geometry of the solid cones in different orientations.

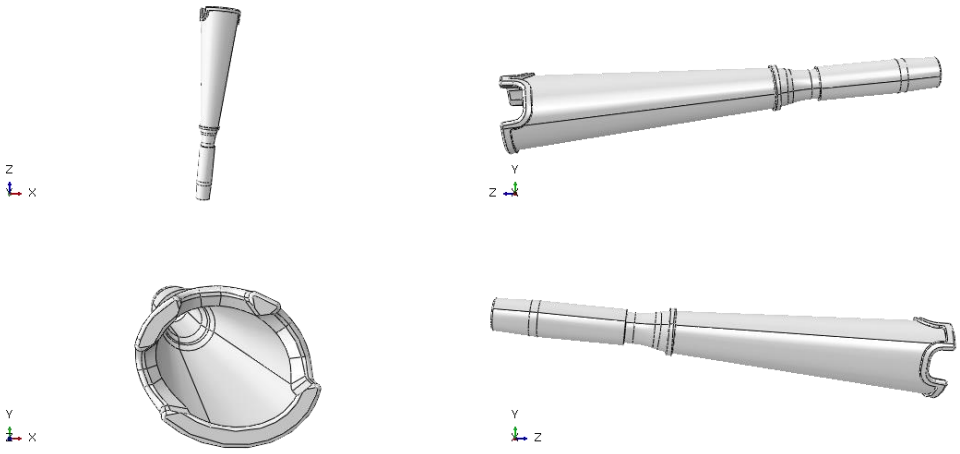

Figure 3.11: Geometry of the porous cones in different orientations.

3.2.1.3. Third Model: R-TKA with press-fit stems

The third model is a traditional revision prosthetic implant that consists of Genus Pantheon hinged prosthesis with press-fit stems, i.e. without cement placed between stem and bone. Press-fit stems differ in geometry in that they have a larger diameter (such that they fill the gaps between bone and stem) and a smaller length (Figure 3.12-a). In this clinical case, however, since the cortical tibia has a proximal part that is really damaged and characterized by massive holes, cement (with properties such that it is a quarter of those of PMMA) was inserted in the proximal part of the tibia in order to fix the stem and not to create gaps in the 3D model. Figure 3.13 shows the presence of cement (in yellow) only in the proximal part of the tibia.

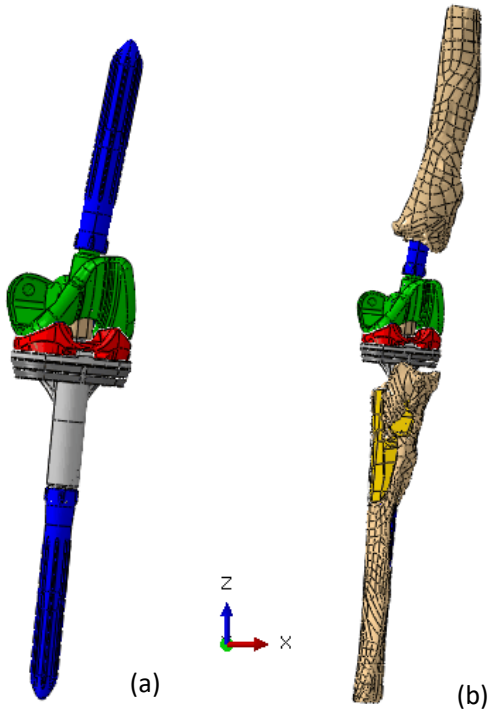

Figure 3.12: Assembly of R-TKA with press-fit stems (a) and of entire third model (b).

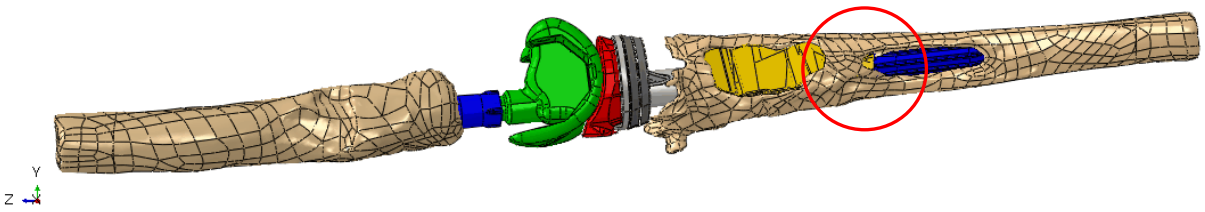

Figure 3.13: Assembly of entire third model in sideways. The red circle highlights the area where the bone cement is cut, and the tibial stem comes into direct contact with the tibia.

3.2.1.4. Fourth Model: R-TKA with cemented stems

The fourth model differs from the third model only in the femoral and tibial stems used. The latter in the fourth model are cemented, i.e. they are designed to be covered with bone cement and do not are in direct contact with the bone. In fact, they have a slightly narrower diameter and slightly greater length than the press-fit stems.

3.2.1.5. Fifth Model: a large resection R-TKA

Finally, the fifth model is a large resection revision TKA (Genus Pantheon hinged prosthesis). It is a prosthesis designed to compensate for significant bone loss and to ensure bone stability in patients requiring radical bone resection. The system consists of femoral component, tibial component, insert, extension piece and cemented stems. The geometry of the femoral component (Figure 3.14-a) and of femoral stem (Figure 3.14-b) appears different from the traditional one, seen in previous models, as there is the presence of the extension piece (Figure 3.14-c). The latter is used to customize the replacement length and attaches a stem to a distal femoral component [59]. In Figure 3.15 is represent the assembly of fifth model in anterior (a) and posterior (b) view, and the assembly of R-TKA in anterior (c) and posterior (d) view.

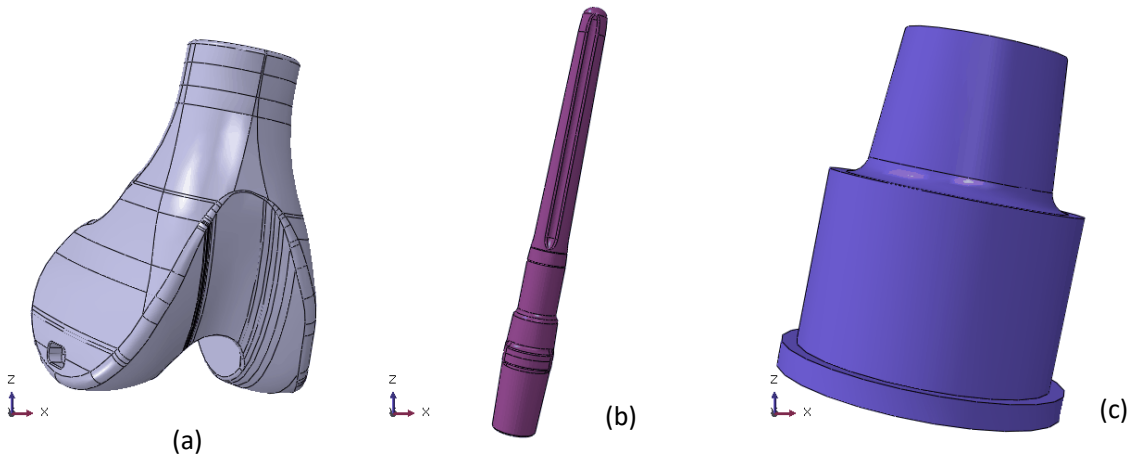

Figure 3.14: The geometry of the femoral component (a), of femoral stem (b) and of the extension piece (c).

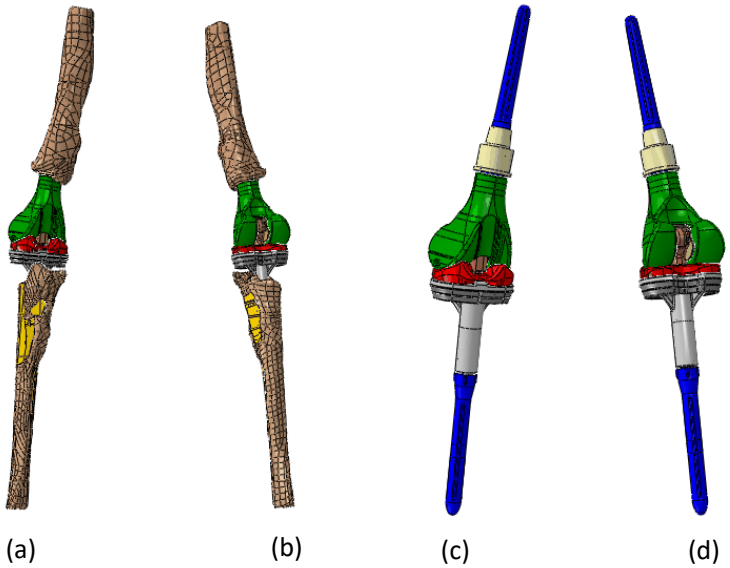

Figure 3.15: Assembly of fifth model in anterior (a) and posterior (b) view, and the assembly of R-TKA in anterior (c) and posterior (d) view.

3.2.2. Material Properties

The materials have been defined and assigned to the corresponding parts through literature research [30,31,46,53-57].

The main properties used to model all the materials are summarized in Table 1.

The femoral components are made of Chromium Cobalt Molybdenum alloy (CoCrMo ISO 5832). The tibial inserts are made of ultra-high molecular weight polyethylene (UHMWPE). The tibial components are made of titanium aluminum vanadium alloy (Ti-6Al-4V ISO 5832-3). All the femoral and tibial stems used are made of titanium aluminum vanadium alloy (Ti-6Al-4V ISO 5832-3). The custom-made bimaterial metaphyseal cones are made of Ti-Por® (marked as Tri-Por material by Adler) and Ti-6Al-4V, and the solid conventional cones are entirely in porous titanium (pure titanium). Instead, the extension piece of fifth model is made of Ti-6Al-4V. According to the literature [29,30,31,34], for all the considered materials, the property of homogeneous, linear elastic isotropic has been optioned, with exception of the cortical bone that is considered linear

transversely isotropic, with the principal axis corresponding to the mechanical axis of the bone (z axis).

Table 1: Material properties and models used for the study.

Material	Material Model	Young's modulus [MPa]	Poisson's ratio	Mass Density [tonn/mm^3]
Cortical bone	Transversely Isotropic	E_1=11 500 E_2=11 500 E_3=17 000	ν_{12}=0.58 ν_{13}=0.31 ν_{23}=0.31	1.85E-09
UHMWPE	Elastic isotropic	685	0.40	9.7E-10
CoCrMo ISO 5832	Elastic isotropic	210 000	0.29	1E-08
Ti6Al-4V ISO 5832-3	Elastic isotropic	110 000	0.35	4.9E-09
Ti-porous	Elastic isotropic	25 000	0.35	4.9E-09
PMMA	Elastic isotropic	3 000	0.35	1.3E-09
Ti-Por®	Elastic isotropic	4865	0,3	2E-09*

For the cortical bone, the direction E3 represents the axial direction.

* Ti-Por® has a density of 42% compared to pure titanium

3.2.3. Load and Boundary Conditions

Two different configurations were considered for all models:

FULL-EXTENSION (0° OF FLEXION)

This configuration reproduces the upright position. The tibia is fixed distally and an axial static load (cranio-caudal direction) of 2200 N is applied on the proximal surface of the femur.

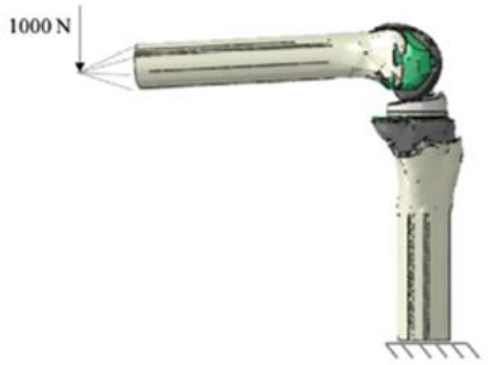

CHAIR-RISE (90° OF FLEXION)

This configuration investigates rising from the seated position. The tibia is fixed distally, and a static load of 1000 N is applied on the proximal surface of the femur in the cranio-caudal direction. The magnitude of the force is reduced in comparison to the other configurations because, usually, a hand support is used during standing up from the sitting position.

These two previous conditions replicated the maximal knee axial force during gait corresponding to about 3.1 times of 70 kg body weight as already implemented in previous studies [31,32-34].

All applied static forces were according to with previous study in the literature [24,29,35-39].

3.2.4. Interactions and Constraints

Since the biomechanical analysis is static, for the simulations, all contact pairs are considered fully bonded, except for the contact pair consisting of the femoral component and tibial insert (for all models) and of all contacts involving cement, such as:

- Contact pair composed from: Cement interposed between stem and cone and stem (for tibia and femur) for 1 and 2 Model;
- Contact pair composed from: Cement interposed between stem and cone and cone (for tibia and femur) for 1 and 2 Model;
- Contact pair composed from: Cement interposed between cone and bone and cone (for tibia and femur) for 1 and 2 Model;

- Contact pair composed from: Cement interposed between cone and bone and bone (for tibia and femur) for 1 and 2 Model;
- Contac pair composed from: Cement and stem (for tibia and for femur) for 3,4, and 5 Model;
- Contac pair composed from: Cement and bone (for tibia and for femur) for 3,4, and 5 Model;

between which friction is present (μ = 0.2) in agreement with previous studies [35].

3.2.5. Mesh settings and Outputs

All the parts of the models were analyzed using finite element analysis (FEA) using linear tetrahedral mesh with the element sizes chosen accordingly to each part. In the relevant part, the size of the mesh elements varies between 1 and 5, and in the other parts between 5 and 10, depending on the geometry. For example, in Figure 3.16 (a) and (b) the tibia mesh and cone mesh appear very dense, unlike the tibial component mesh which is less dense (Figure 3.16-c). A proper mesh quality was ensured through convergence analysis [40].

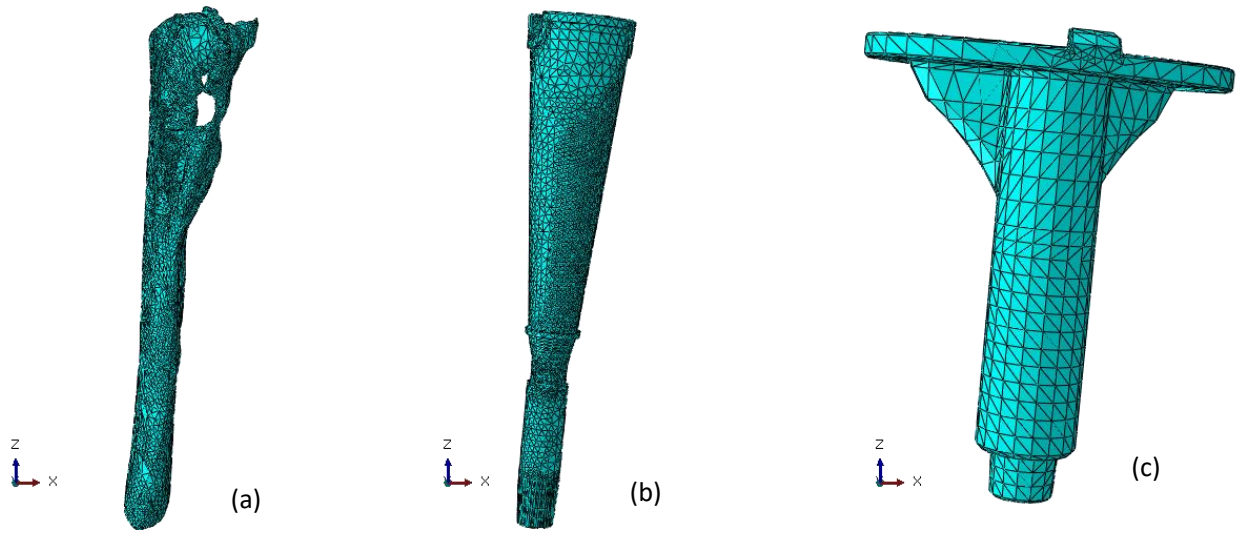

Figure 3.16: Example of the mesh element's size of tibia (a), cone (b), and tibial component (c).

The Outputs observed were Stress Contours (**Distribution of Von Mises Stress** in the bones) and the **risk of fracture** (RF). The RF of bones was calculated considering similar studies in the literature [41,42]. Initially, the maximum strain was calculated by dividing the maximum (tensile) and minimum (compressive) stresses along the principal axis direction by the component of the elastic modulus of cortical bone along the same direction (E3). After that, the maximum strain obtained for tension and compression ($\varepsilon_{max\text{-}tensile}$ and $\varepsilon_{max\text{-}compressive}$, respectively) was divided by the ultimate strain limit (0.0073 and 0.0104, respectively) [41,42]. Finally, the maximum value is chosen from the two.

$$RF = \frac{\varepsilon\_\max}{\varepsilon\_lim}$$

The biomechanical results will be shown in detail in the next chapter.

Chapter 4

Biomechanical Results

As already mentioned in the previous chapter, when discussing and analyzing the biomechanical results obtained, it is possible to distinguish between qualitative and quantitative analysis.

4.1. Qualitative Analysis

The Figure 4.1 shows qualitative trends of femur and tibia for full-extension configuration in anterior view:

FULL-EXT	BIMATERIAL CONE	SOLID CONE	PRESS-FIT STEM	CEMENTED STEM	LARGE RESECTION
Femur	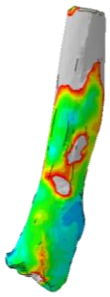	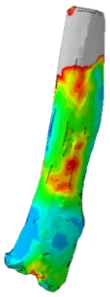	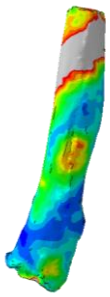	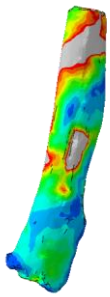	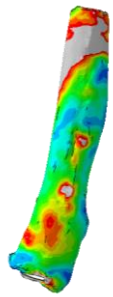
Tibia	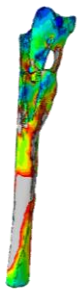	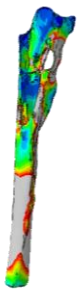	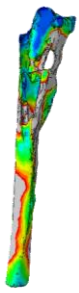	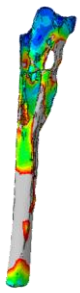	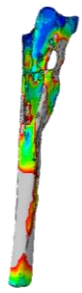

Figure 4.1: Graphical anterior view of the von Mises stress for the full-extension configuration. Each column represents the values for each technique analyzed, while, the rows indicate the different bones modelled.

The Figure 4.2 shows qualitative trends of bones for full-extension configuration in posterior view:

FULL-EXT	BIMATERIAL CONE	SOLID CONE	PRESS-FIT STEM	CEMENTED STEM	LARGE RESECTION
Femur	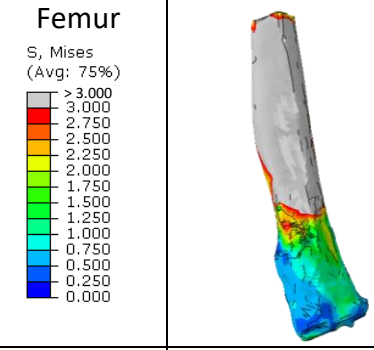	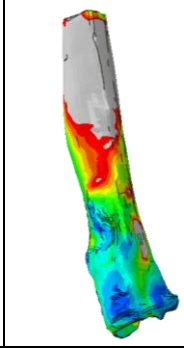	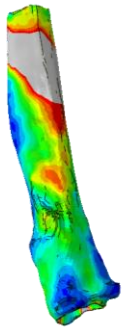	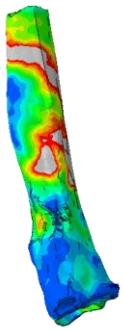	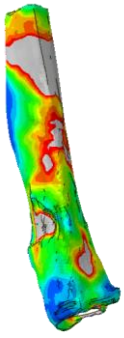
Tibia	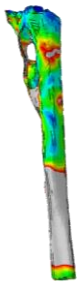	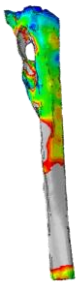	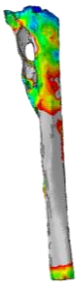	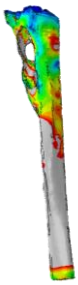	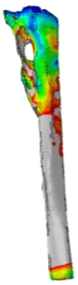

Figure 4.2: Graphical posterior view of the von Mises stress for the full-extension configuration. Each column represents the values for each technique analyzed, while the rows indicate the different bones modelled.

The Figure 4.3 shows qualitative trends of bones for chair-rise configuration in anterior view:

CHAIR-RISE	BIMATERIAL CONE	SOLID CONE	PRESS-FIT STEM	CEMENTED STEM	LARGE RESECTION
Femur		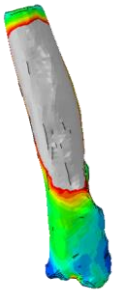		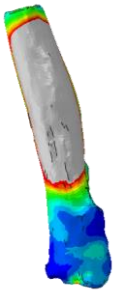	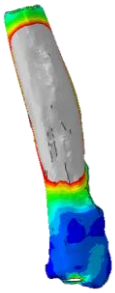
Tibia	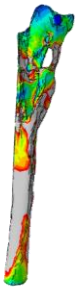	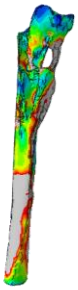	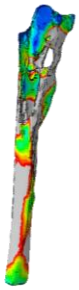		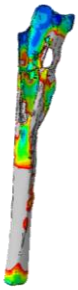

Figure 4.3: Graphical anterior view of the von Mises stress for the chair-rise configuration. Each column represents the values for each technique analyzed, while the rows indicate the different bones modelled.

The Figure 4.4 shows qualitative trends of femur and tibia for chair-rise configuration in posterior view:

CHAIR-RISE	BIMATERIAL CONE	SOLID CONE	PRESS-FIT STEM	CEMENTED STEM	LARGE RESECTION
Femur	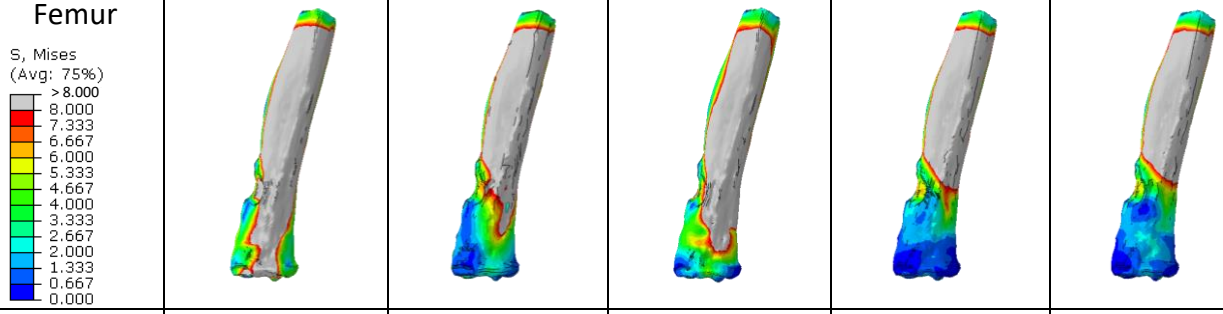				
Tibia	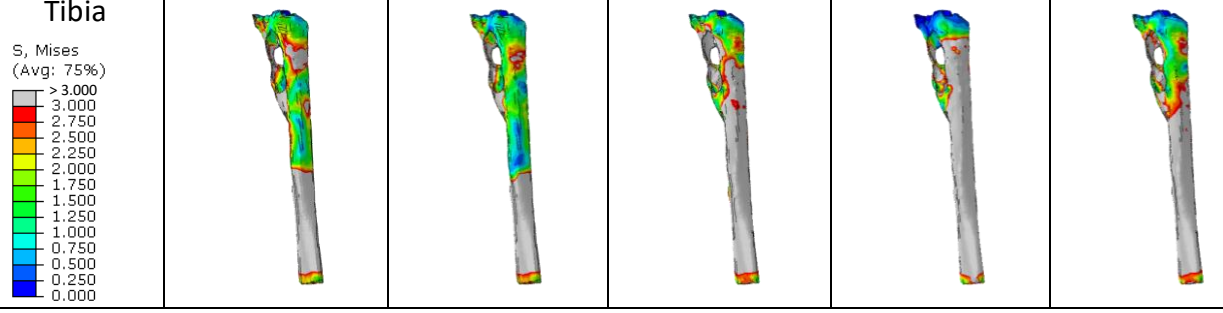				

Figure 4.4: Graphical posterior view of the von Mises stress for the chair-rise configuration. Each column represents the values for each technique analyzed, while, the rows indicate the different bones modelled.

The Figure 4.5 shows qualitative trends of tibia in superior view, for both configurations analyzed:

TIBIA	BIMATERIAL CONE	SOLID CONE	PRESS-FIT STEM	CEMENTED STEM	LARGE RESECTION
FULL-EXT	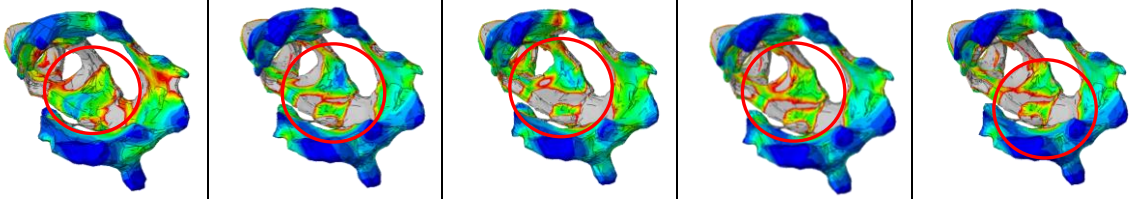				
CHAIR-RISE	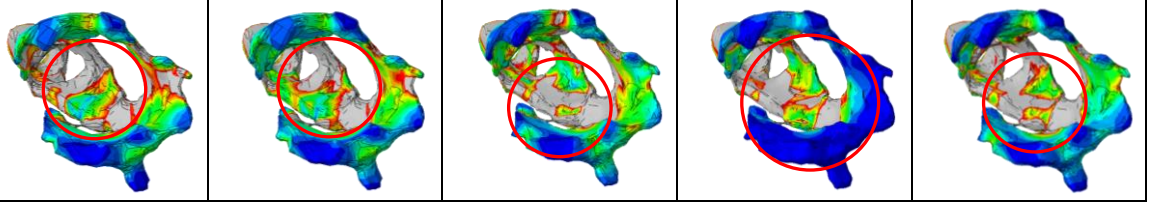				

Figure 4.3: Graphical overview of the von Mises stress for tibia, in superior view. Each column represents the values for each technique analyzed, while, the rows indicate the different configurations analyzed.

4.2. Quantitative Analysis

The following tables show the relative bone fracture risk in percentage value for the two configurations analyzed.

Table 2: Risk of Fracture in % for full-extension configuration, for Femur and Tibia.

FULL-EXT	Bimaterial cone	Solid cone	Press-fit stem	Cemented stem	Large resection
Femur	1,474	1,212	6,700	0,327	1,423
Tibia	3,123	2,708	1,734	3,008	2,917

Table 3: Risk of Fracture in % for chair-rise configuration, for Femur and Tibia.

CHAIR-RISE	Bimaterial cone	Solid cone	Press-fit stem	Cemented stem	Large resection
Femur	0,758	1,619	3,209	0,178	0,478
Tibia	0,793	1,492	0,704	0,207	1,287

4.3. Comparison

In general, the use of custom-made cones (first and second models) leads to more similar results compared to the other techniques used.

Figure 4.1 and Figure 4.2 show the qualitative trends for the patient's bones in the full-extension configuration. It is important to specify that the proximal part of both the femur and the tibia is more affected (areas in red) due to the static load of 2200 N applied in those areas.

In general, when observing full extension under load, the technique used in the first and second models better distributes the stress, generating a homogeneous stress contour on both bones, while the other three techniques concentrate the stress in specific regions. Regarding the femur in the full-extension configuration, we can observe how the custom-made cone correctly and uniformly

applies stress to the distal part of the femur. On the other hand, the presence of the stem induces stress shielding because the axial load applied to the femoral head, due to the inadequate implant design, is primarily transferred to the implant, and the bone, receiving minimal load, can undergo degeneration (the femur tends to resorb). Stress shielding is induced especially in the case of the press-fit stem. Furthermore, the large resection applies stress, but since the distribution is discontinuous, this can lead to local stress peaks that could result in bone fractures.

As observed for full extension, for the other simulated daily activity (chair-rise) shown in Figure 4.3 and Figure 4.4, the use of a custom-made cone also induces a more homogeneous stress distribution. Specifically, the stress in the distal femur is uniform with the custom-made cones having higher stress levels in the case of Ti-Por (green/yellow zones). The press-fit stem induces high stress up to the proximal zone with a risk of fracture. On the other hand, the cemented stem and the large resection induce stress shielding in the distal femur.

As far as the tibia is concerned, in both full extension and chair-rise configurations, as shown in Figure 4.6, a better distribution is observed in revision techniques with custom-made cones, compared to traditional revision techniques in which areas of higher (in red) and lower (in blue) stress alternate in the same area.

In addition, to quantify the possible bone overload induced by the different techniques, the fracture risk for full-extension (Table 2) and chair-rise (Table 3) was calculated for the tibia and femur for each technique [41,42]. In detail, a value of 100% (or higher) indicates a fracture, while lower values indicate a lower probability of fracture. Figures 4.6 and 4.7 show the same values for the full-extension and chair-rise configuration respectively in the form of a histogram to better capture the differences between the techniques analyzed. In general, the use of cement (fourth model) confirms the results of the literature studies in preventing the risk of bone fracture [35] with the lowest values reported, for both tibia and femur, among the configurations examined; the first, the second and

fifth models have very similar results, while the third model (press-fit stems) reported the highest risk of fracture, in agreement with other biomechanical studies [29,43].

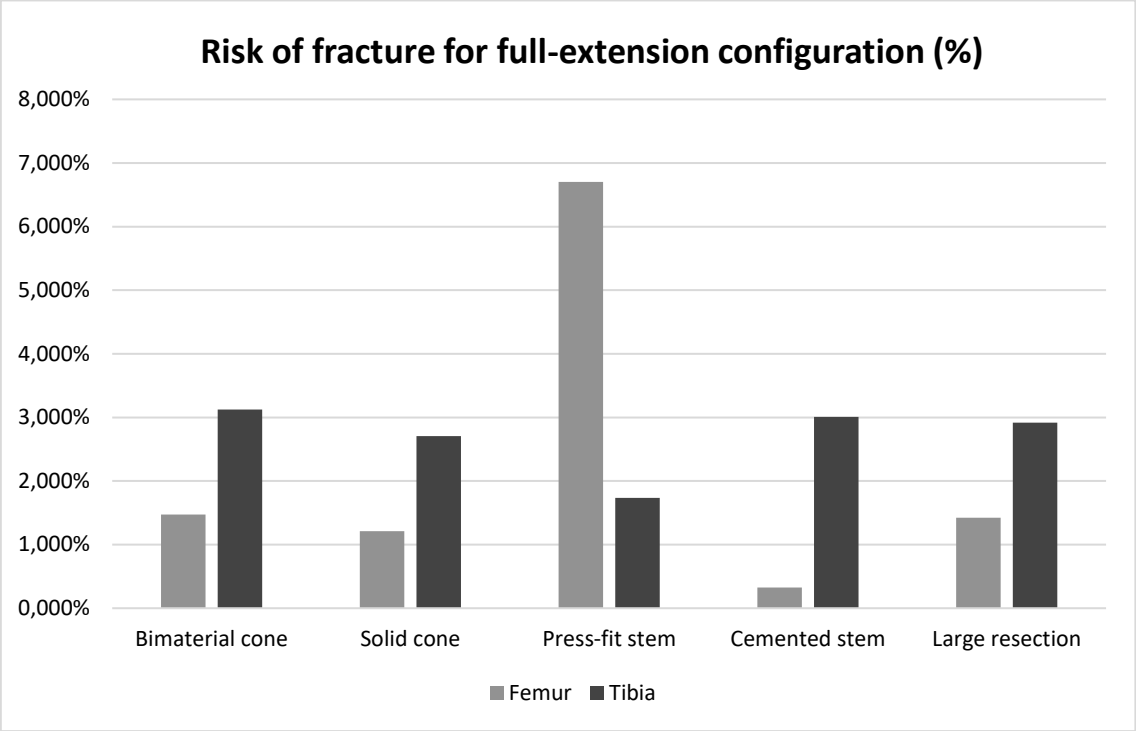

Figure 4.6: Comparison of the risk of fracture, expressed in %, calculated for each technique and for full-extension configuration.

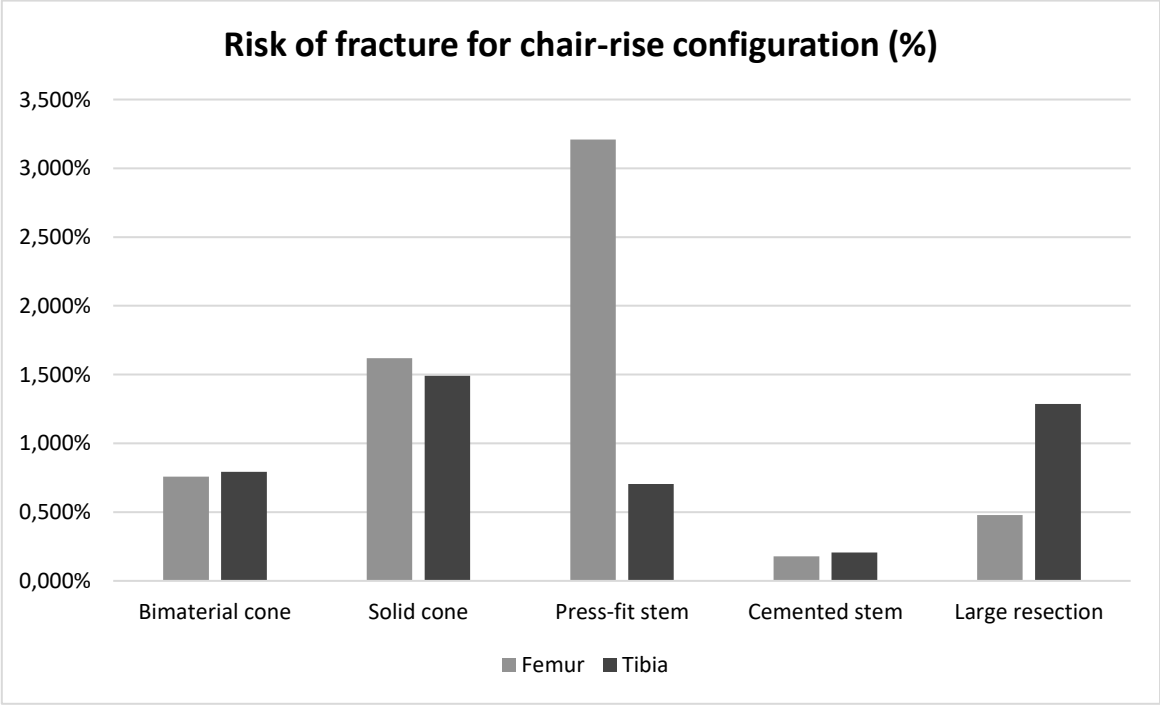

Figure 4.7: Comparison of the risk of fracture, expressed in %, calculated for each technique and for chair-rise configuration.

4.4. Discussion

The management of significant losses of bone tissue is one of the primary challenges in knee revision surgery [44,48]. Custom-made cones represent a new and promising option in this surgical context. This biomechanical analysis has reported optimal results for a range of patients with severe distal femoral and/or tibial bone losses so extensive that the use of standard cones to stabilize the implant is not advisable. These findings are supported by other biomechanical studies in the literature, and the authors have reported promising short-term clinical data on patient-specific titanium cones without radiological or clinical complications [45,46].

In a TKA (Total Knee Arthroplasty) revision, prosthetic stability is crucial and can be compromised when dealing with extremely weak and fragile bones. Porous metal custom-made cones provide reliable stability in the meta-diaphyseal region, involving a "new" area for implant fixation midway between purely metaphyseal and purely diaphyseal regions. Consequently, custom devices should be considered as an intermediate option between "off-the-shelf" metaphyseal fixation tools and massive bone resection with mega prosthesis implantation. Given the positive clinical outcomes (excellent patient physical conditions), this analysis provides a biomechanical explanation for understanding the effects when using custom meta-diaphyseal cones in severe knee arthroplasty revisions [46].

This study presents the results of a finite element analysis on a patient who received a revision implant with custom-made cones. The surgical approach was compared to a similar situation involving the use of solid cones and traditional knee revision approaches.

The results confirm those obtained in other biomechanical studies in the literature [45,46,48,49]. In both the first and second techniques that used the custom cones, the stress distribution appears to be uniform, reducing the risk of loosening.

The presence of porous custom-made cones in revision implants reduces the risk of stress shielding, transfers loads to the bone, and increases implant stability. These findings can be justified by the fact that the material used for custom-made cones, porous titanium, [50,55,85], has mechanical properties better suited to the needs of this study compared to other materials. Additionally, the custom prosthesis geometry fits the patient's anatomy more effectively.

Through the qualitative trends of the bone in both configurations, we observe the advantage of custom bimaterial cones over solid cones. Since the proximal area of the femur and tibia (the one near the implant) appears to be more stressed with the first technique than with the second, this implies better osseointegration and reduced rejection of the host object by the bone, thanks to the presence of trabecular titanium [51, 82-85]. The physiologic distribution could prevent the patient from feeling pain and from the risk of loosening. Moreover, a low stress gradient improving implant stability and inducing a lower risk of bone fractures. These results could be estimated as in agreement with other literature studies [46].

Regarding techniques C and D, similar trends for stress induced by cemented or press-fit stem can be found in the literature [29, 35] and consensus on improved behavior on bone-metal interface when porous metal is also reported in the literature [30]. The higher stress on the proximal bone especially induced by the press-fit technique could alter the bone remodeling as it induces stress shielding [43,44,52].

Lastly, to establish the potential for femoral bone fracture under the different loading conditions, a risk for fracture (RF) was therefore calculated. The latter is lower in R-TKA with the use of cemented stems; similar results are obtained with the use of the cone and the large resection prosthesis. In contrast, in the implant with press-fit stems the percentage values for RF are significantly higher. Again, the results agree with those of other biomechanical studies [29,35,43].

The limitations of the study are however noteworthy, mainly related to the fact that only a static and not a dynamic analysis was conducted; however, two loading configurations with five different surgical approaches used for severe revisions were analyzed. All material models are considered elastically linear, soft tissue and patella were not actually implemented in the model, but their contribution was nevertheless included in the boundary conditions [24,29,30]. These abbreviations adopted are commonly accepted in various studies in the literature [31,32,33,34,37].

Chapter 5

Conclusion

In recent years, the use of additive manufacturing technology has significantly increased in various manufacturing sectors for the production of complex-geometry artifacts and components.

In the biomedical sector, in particular, the use of this technology allows for the creation of cellular solids in metallic biomaterials that can strongly contribute to the osseointegration of orthopedic implants while maintaining good mechanical properties.

Various studies have been conducted on biomedical applications using titanium and its alloys as materials for prosthetic components obtained through powder-based technology [82-84]. This enables the fabrication of trabecular titanium structures with a low elastic modulus, easily comparable to the values of cancellous bone and much lower than those for cortical bone. This is due to the high level of porosity in these structures.

Based on previous studies in the literature, additive manufacturing technology is capable of developing implants with materials like titanium that facilitate osseointegration and bone remodeling, and more. Thanks to powder-based technology, it's possible to obtain not only components made of trabecular metal but also highly complex structures that adapt to the patient's anatomy, namely custom-made implants [45,48,49]. Therefore, it has also been used to design prosthetic components for revision implants, which are different from traditional ones and can adapt to the anatomy of patients with significant bone defects.

Thus, the creation of a patient-specific cone designed through the 3D reconstruction of the patient's anatomy derived from tomographic images with porosity tailored to the patient's bone conditions (the first model analyzed in this biomechanical analysis) can only bring further advantages.

This study aimed to understand the benefits obtained from the use of custom-made cones (both in Ti-Por ® and conventional porous titanium) compared to the performance of traditional techniques, such as the use of cemented or uncemented stems or extensive resection.

Following the qualitative results obtained from the numerical biomechanical analysis, it can be confirmed that the presence of porous custom-made cones leads to a homogeneous distribution of stresses and a lower stress gradient on the bones, which could reduce the probability of bone fractures around the implant and the likelihood of implant mobilization once a custom-made porous cone is used. Furthermore, the absence of stress peaks may be associated with a potential reduction in perceived pain.

Finally, to underscore the advantage induced by the use of porous titanium cones compared to solid porous titanium cones, this study could be enhanced by conducting quantitative analysis in regions of interest, such as the proximal part of the bones.

References

[1] Hirschmann MT, Müller W. Complex function of the knee joint: the current understanding of the knee. Knee Surg Sports Traumatol Arthrosc. 2015 Oct;23(10):2780-8. doi: 10.1007/s00167-015-3619-3. Epub 2015 May 12. PMID: 25962963.

[2] J. G. Betts et al., Anatomy and Physiology. 2013.

[3] Hsu H, Siwiec RM. Knee Arthroplasty. 2023 Jul 24. In: StatPearls [Internet]. Treasure Island (FL): StatPearls Publishing; 2023 Jan–. PMID: 29939691.

[4] S. Affatato, 2 - Biomechanics of the knee, Editor(s): Saverio Affatato, Surgical Techniques in Total Knee Arthroplasty and Alternative Procedures, Woodhead Publishing, 2015, Pages 17-35, ISBN 9781782420309, https://doi.org/10.1533/9781782420385.1.17.

[5] Bozkurt, Murat & Acar, Halil. (2021). Clinical Anatomy of the Knee An Atlas: An Atlas. 10.1007/978-3-030-57578-6.

[6] Innocenti, Bernardo & Bori, Edoardo & Piccolo, Stephane. (2020). Development and validation of a robust patellar reference coordinate system for biomechanical and clinical studies. The Knee. 27. 10.1016/j.knee.2019.09.007.

[7] Fox AJ, Bedi A, Rodeo SA. The basic science of human knee menisci: structure, composition, and function. Sports Health. 2012 Jul;4(4):340-51. https://doi: 10.1177/1941738111429419. PMID: 23016106; PMCID: PMC3435920.

[8] Abulhasan, J.F.; Grey, M.J. Anatomy and Physiology of Knee Stability. *J. Funct. Morphol. Kinesiol.* 2017, *2*, 34. https://doi.org/10.3390/jfmk2040034.

[9] Yazdi H, Nazarian A, Kwon JY, Hochman MG, Pakdaman R, Hafezi P, Ghahremani M, Joudi S, Ghorbanhoseini M. Anatomical axes of the proximal and distal halves of the femur in a normally aligned healthy population: implications for surgery. J Orthop Surg Res. 2018 Jan 31;13(1):21. doi: 10.1186/s13018-017-0710-0. PMID: 29386019; PMCID: PMC5793359.

[10] S.D. Masouros, A.M.J. Bull, A.A. Amis, (i) Biomechanics of the knee joint, Orthopaedics and Trauma, Volume 24, Issue 2, 2010, Pages 84-91, ISSN 1877-1327, https://doi.org/10.1016/j.mporth.2010.03.005.

[11] Johal P, Williams A, Wragg P, Hunt D, Gedroyc W. Tibio-femoral movement in the living knee. A study of weight bearing and non-weight bearing knee kinematics using 'interventional' MRI. J Biomech. 2005 Feb;38(2):269-76. doi: 10.1016/j.jbiomech.2004.02.008. PMID: 15598453.

[12] Rivière Charles and Vendittoli Pascal-André, *Personalized Hip and Knee Joint Replacement*. 2020.

[13] Blackburne J, Peel T. A new method of measuring patellar height. J Bone Joint Surg Br. 1977;59-B (2):241-242. doi:10.1302/0301-620X.59B2.873986.

[14] Luyckx T, Didden K, Vandenneucker H, Labey L, Innocenti B, Bellemans J. Is there a biomechanical explanation for anterior knee pain in patients with patella alta?: influence of patellar height on patellofemoral contact force, contact area and contact pressure. J Bone Joint Surg Br. 2009 Mar;91(3):344-50. doi: 10.1302/0301-620X.91B3.21592. PMID: 19258610.

[15] Wilcox RB, Arslanian LE, Millett P. Rehabilitation following total shoulder arthroplasty. J Orthop Sports Phys Ther. 2005 Dec;35(12):821-36. doi: 10.2519/jospt.2005.35.12.821. PMID: 16848103.

[16] Filbay SR, Grindem H. Evidence-based recommendations for the management of anterior cruciate ligament (ACL) rupture. Best Pract Res Clin Rheumatol. 2019 Feb;33(1):33-47. doi: 10.1016/j.berh.2019.01.018. Epub 2019 Feb 21. PMID: 31431274; PMCID: PMC6723618.

[17] Schenkman M, Rugo de Cartaya V. Kinesiology of the shoulder complex. J Orthop Sports Phys Ther. 1987;8(9):438-50. doi: 10.2519/jospt.1987.8.9.438. PMID: 18797034.

[18] Legnani G., Palmieri G., Fondamenti di meccanica e biomeccanica del movimento. Milano. Città studi edizioni. 2016.

[19] Blalock D, Miller A, Tilley M, Wang J. Joint instability, and osteoarthritis. Clin Med Insights Arthritis Musculoskelet Disord. 2015 Feb 19; 8:15-23. doi: 10.4137/CMAMD.S22147. PMID: 25741184; PMCID: PMC4337591.

[20] Murphy NJ, Eyles JP, Hunter DJ. Hip Osteoarthritis: Etiopathogenesis and Implications for Management. Adv Ther. 2016 Nov;33(11):1921-1946. doi: 10.1007/s12325-016-0409-3. Epub 2016 Sep 26. PMID: 27671326; PMCID: PMC5083776.

[21] Kurtz SM, Ong KL, Lau E, Widmer M, Maravic M, Gómez-Barrena E, de Pina Mde F, Manno V, Torre M, Walter WL, de Steiger R, Geesink RG, Peltola M, Röder C. International survey of primary and revision total knee replacement. Int Orthop. 2011 Dec;35(12):1783-9. doi: 10.1007/s00264-011-1235-5. Epub 2011 Mar 15. PMID: 21404023; PMCID: PMC3224613.

[22] Hussain, M.; Naqvi, R.A.; Abbas, N.; Khan, S.M.; Nawaz, S.; Hussain, A.; Zahra, N.; Khalid, M.W. Ultra-High-Molecular-Weight-Polyethylene (UHMWPE) as a Promising Polymer Material for Biomedical Applications: A Concise Review. *Polymers* 2020, *12*, 323. https://doi.org/10.3390/polym12020323.

[23] Bourdon CE, Broberg JS, McCalden RW, Naudie DD, MacDonald SJ, Lanting BA, Teeter MG. Comparison of long-term kinematics and wear of total knee arthroplasty implant designs. J Mech Behav Biomed Mater. 2021 Dec; 124:104845. doi: 10.1016/j.jmbbm.2021.104845. Epub 2021 Sep 20. PMID: 34555623.

[24] Innocenti, Bernardo. (2019). High congruency MB insert design: stabilizing knee joint even with PCL deficiency. Knee Surgery, Sports Traumatology, Arthroscopy. 28. 10.1007/s00167-019-05764-0.

[25] Mazzucchelli L, Deledda D, Rosso F, Ratto N, Bruzzone M, Bonasia DE, Rossi R. Cruciate retaining and cruciate substituting ultra-congruent insert. Ann Transl Med. 2016 Jan;4(1):2. doi: 10.3978/j.issn.2305-5839.2015.12.52. PMID: 26855938; PMCID: PMC4716943.
[26] Sabatini, Luigi & Risitano, Salvatore & Rissolio, Lorenzo & Bonani, Andrea & Atzori, F. & Massè, Alessandro. (2017). Condylar constrained system in primary total knee replacement: Our experience and literature review. Annals of Translational Medicine. 5. 135-135. 10.21037/atm.2017.03.29.

[27] Athwal KK, Willinger L, Manning W, Deehan D, Amis AA. A constrained-condylar fixed-bearing total knee arthroplasty is stabilised by the medial soft tissues. Knee Surg Sports Traumatol Arthrosc. 2021 Feb;29(2):659-667. doi: 10.1007/s00167-020-05995-6. Epub 2020 Apr 22. PMID: 32322947; PMCID: PMC7892729.

[28] Chang C, Lai K, Yang C, Lan S. Early mechanical complications of a multidirectional mobile-bearing total knee replacement. J Bone Joint Surg Br. 2011;93-B (4):479-483. doi: 10.1302/0301-620X.93B4.25864.

[29] Andreani L, Pianigiani S, Bori E, Lisanti M, Innocenti B (2020) Analysis of biomechanical differences between condylar constrained knee and rotating hinged implants: a numerical study. J Arthroplasty. https ://doi.org/10.1016/j.arth.2019.08.005.

[30] Castellarin, G., Pianigiani, S., & Innocenti, B. (2019). Asymmetric polyethylene inserts promote favorable kinematics and better clinical outcome compared to symmetric inserts in a mobile bearing total knee arthroplasty. *Knee surgery, sports traumatology, arthroscopy: official journal of the ESSKA*, *27*(4), 1096–1105. https://doi.org/10.1007/s00167-018-5207-9.

[31] Innocenti B, Fekete G, Pianigiani S. Biomechanical Analysis of Augments in Revision Total Knee Arthroplasty. J Biomech Eng. 2018 Nov 1;140(11):111006. doi: 10.1115/1.4040966. PMID: 30098138.

[32] Innocenti B, Bilgen OF, Labe L, van Lenth GH, Slote JV, Catani F (2014) Load sharing and ligament strains in balanced, overstuffed and understuffed UKA. A validated finite element analysis. J Arthroplasty. https ://doi.org/10.1016/j.arth.2014.01.020.

[33] Innocenti B, Bellemans J, Catani F (2015) Deviations from optimal alignment in TKA: is there a biomechanical difference between femoral or tibial component alignment? J Arthroplasty. https ://doi.org/10.1016/j.arth.2015.07.038.

[34] Innocenti B, Pianigiani S, Ramundo G, Thienpont E (2016) Biomechanical effects of different varus and valgus alignments in medial unicompartmental knee arthroplasty. J Arthroplasty 31(12):2685–2691.

[35] El-Zayat BF, Heyse TJ, Fanciullacci N, Labey L, Fuchs-Winkelmann S, Innocenti B (2016) Fixation techniques and stem dimensions in hinged total knee arthroplasty: a finite element study. Arch Orthop Trauma Surg. https ://doi.org/10.1007/s00402-016-2571-0.

[36] Belvedere C, Leardini A, Catani F, Pianigiani S, Innocenti B (2017) In vivo kinematics of knee replacement during daily living activities: condylar and post-cam contact assessment by three-dimensional fluoroscopy and finite element analyses. J Orthop Res.
https ://doi.org/10.1002/jor.23405.

[37] Brihault J, Navacchia A, Pianigiani S, Labey L, De Corte R, Pascale V, Innocenti B (2016) All-polyethylene tibial components generate higher stress and micromotions than metal-backed tibial components in total knee arthroplasty. Knee Surg Sports TraumatolArthrosc.
https ://doi.org/10.1007/s0016 7-015-3630-8.

[38] Innocenti B, Robledo Yagüe H, AlarioBernabé R, Pianigiani S (2015) Investigation on the effects induced by TKA features on tibio-femoral mechanics part I: femoral component designs. J Mech Med Biol. https ://doi.org/10.1142/S0219 51941 54003 45.

[39] Pianigiani S, AlarioBernabé R, Robledo Yagüe H, Innocenti B (2015) Investigation on the effects induced by TKA features on tibio-femoral mechanics part II: tibial insert designs. J Mech Med Biol.
https ://doi.org/10.1142/S0219 51941 54003 57.

[40] Pianigiani S, Innocenti B (2015) The use of finite element modeling to improve biomechanical research on knee prosthesis. In: Stewart J (ed) New developments in knee prosthesis research. Nova Science Publishers, Hauppauge, NY, pp 113–126.

[41] Soenen M, Baracchi M, De Corte R, Labey L, Innocenti B (2013) Stemmed TKA in a femur with a total hip arthroplasty: is there a safe distance between the stem tips? J Arthroplasty. https ://doi. org/10.1016/j.arth.2013.01.010.

[42] Schileo E, Dall'Ara E, Taddei F, Malandrino A, Schotkamp T, Baleani M, Viceconti M (2008) An accurate estimation of bone density improves the accuracy of subject-specific finite element models. J Biomech. https ://doi.org/10.1016/j.jbiomech.2008.05.017.

[43] Completo A, Talaia P, Fonseca F, Simões JA (2009) Relationship of design features of stemmed tibial knee prosthesis with stress shielding and end-of-stem pain. Mater Des. https ://doi. org/10.1016/j.jbiom ech.2007.10.006.

[44] Burastero G, Cavagnaro L, Chiarlone F, Alessio-Mazzola M, Carrega G, Felli L (2018) The use of tantalum metaphyseal cones for the management of severe bone defects in septic knee revision. J Arthroplasty. https ://doi.org/10.1016/j.arth.2018.08.026.

[45] Cherny AA, Kovalenko AN, Bilyk SS, Denisov AO, Kazemirskiy AV, Kulyaba TA, Kornilov NN (2019) Early outcomes of patient-specific modular cones for substitution of methaphysial and diaphyseal bone defects in revision knee arthroplasty. Travmatologiya i ortopediyaRossii Traumatology and Orthopedics of Russia. https ://doi.org/10.21823 /2311-2905-2019-25-2-9-18.

[46] Burastero G, Pianigiani S, Zanvettor C, Cavagnaro L, Chiarlone F, Innocenti B. Use of porous custom-made cones for meta-diaphyseal bone defects reconstruction in knee revision surgery: a clinical and biomechanical analysis. *Arch Orthop Trauma Surg*. 2020;140(12):2041-2055.
https ://doi.org/10.1007/s00402-020-03670-6.

[47] Morgan-Jones R, Oussedik SIS, Graichen H, Haddad FS (2015) Zonal fixation in revision total knee arthroplasty. Bone Jt J. https://doi.org/10.1302/0301-620X.97B2.34144.

[48] Burastero, Giorgio & Cavagnaro, Luca & Chiarlone, Francesco & Innocenti, Bernardo & Felli, Lamberto. (2018). A Case Report: Custom Made Porous Titanium Implants in Revision: A New Option for Complex Issues. The Open Orthopaedics Journal. 12. 525-535. 10.2174/1874325001812010525.

[49] Ahmad Faizan, Manoshi Bhowmik-Stoker, Vincent Alipit, Amanda E. Kirk, Viktor E. Krebs, Steven F. Harwin, R. Michael Meneghini, Development and Verification of Novel Porous Titanium Metaphyseal Cones for Revision Total Knee Arthroplasty, The Journal of Arthroplasty, Volume 32, Issue 6, 2017, Pages 1946-1953, ISSN 0883-5403, https://doi.org/10.1016/j.arth.2017.01.013.

[50] Pałka, Krzysztof, and Rafał Pokrowiecki. "Porous titanium implants: a review." *Advanced Engineering Materials* 20.5 (2018): 1700648. https://doi.org/10.1002/adem.201700648.

[51] Lachiewicz PF, Watters TS. Porous metal metaphyseal cones for severe bone loss. Bone Joint J. 2014;96-B(11_Supple_A):118-121. doi:10.1302/0301-620X.96B11.34197.

[52] Abraham R, Malkani AL, Lewis J, Beck D (2007) An anatomical study of tibial metaphyseal/diaphyseal mismatch during revision total knee arthroplasty. J Anthroplasty. https ://doi.org/10.1016/j. arth.2006.06.001.

[53] Andreani, L., Pianigiani, S., Bori, E., Lisanti, M., & Innocenti, B. (2020). Analysis of Biomechanical Differences Between Condylar Constrained Knee and Rotating Hinged Implants: A Numerical Study. *The Journal of arthroplasty*, *35*(1), 278–284. https://doi.org/10.1016/j.arth.2019.08.005.

[54] Bernardo Innocenti, Silvia Pianigiani, Gaetano Ramundo, Emmanuel Thienpont, Biomechanical Effects of Different Varus and Valgus Alignments in Medial Unicompartmental Knee Arthroplasty, The Journal of Arthroplasty, Volume 31, Issue 12, 2016, Pages 2685-2691, ISSN 0883-5403, https://doi.org/10.1016/j.arth.2016.07.006.

[55] Marin, Elia & Lanzutti, Alex & Turchet, S. & Fusi, S. & Pressacco, Michele & Fedrizzi, L. (2011). Structural and mechanical characterization of highly porous biomaterials in commercially pure titanium for orthopaedic arthroplasty: Trabecular TitaniumTM. Metallurgia Italiana. 103. 27-36.

[56] Singh, S., & Harsha, A. P. (2016). Analysis of femoral components of cemented total hip arthroplasty. *Journal of The Institution of Engineers (India): Series D*, *97*, 113-120.

[57] Bori, E., Armaroli, F., & Innocenti, B. (2022). Biomechanical analysis of femoral stems in hinged total knee arthroplasty in physiological and osteoporotic bone. *Computer methods and programs in biomedicine*, *213*, 106499. https://doi.org/10.1016/j.cmpb.2021.106499.

[58] Calori, G.M., Mazza, E., Bucci, M. *et al.* Megaprotesi in acuto e negli esiti traumatici degli arti. *LO SCALPELLO* 29, 237–245 (2015). https://doi.org/10.1007/s11639-015-0136-6.

[59] https://www.stryker.com/it/it/joint-replacement/products/gmrs/index-eu.html.

[60] Beckmann, N. A., Mueller, S., Gondan, M., Jaeger, S., Reiner, T., & Bitsch, R. G. (2015). Treatment of severe bone defects during revision total knee arthroplasty with structural allografts and porous metal cones-a systematic review. *The Journal of arthroplasty*, *30*(2), 249–253. https://doi.org/10.1016/j.arth.2014.09.016.

[61] Chokhandre, S., Schwartz, A., Klonowski, E., Landis, B., & Erdemir, A. (2023). Open Knee(s): A Free and Open Source Library of Specimen-Specific Models and Related Digital Assets for Finite Element Analysis of the Knee Joint. *Annals of biomedical engineering*, *51*(1), 10–23. https://doi.org/10.1007/s10439-022-03074-0.

[62] Loi, I., Stanev, D., & Moustakas, K. (2021). Total knee replacement: subject-specific modeling, finite element analysis, and evaluation of dynamic activities. *Frontiers in Bioengineering and Biotechnology*, *9*, 648356.

[63] Kluess, D. (2010). Finite element analysis in orthopaedic biomechanics. In *Finite element analysis*. IntechOpen.

[64] Moiduddin K, Mian SH, Umer U, Alkhalefah H, Ahmed F, Hashmi FH. Design, Analysis, and 3D Printing of a Patient-Specific Polyetheretherketone Implant for the Reconstruction of Zygomatic Deformities. *Polymers*. 2023; 15(4):886. https://doi.org/10.3390/polym15040886.

[65] Benca, E., Amini, M. & Pahr, D.H. Effect of CT imaging on the accuracy of the finite element modelling in bone. *Eur Radiol Exp* 4, 51 (2020). https://doi.org/10.1186/s41747-020-00180-3.

[66] Singh, P. (2017). A Ct Scan Based Cad Modeling of A Human Femur Coupled With Fe Analysis. https://api.semanticscholar.org/CorpusID:212435234.

[67] Lee, Y. S., & Chen, A. F. (2018). Two-Stage Reimplantation in Infected Total Knee Arthroplasty. *Knee surgery & related research*, *30*(2), 107–114. https://doi.org/10.5792/ksrr.17.095.

[68] Migliorini, F., Maffulli, N., Cuozzo, F., Pilone, M., Elsner, K., & Eschweiler, J. (2022). No difference between mobile and fixed bearing in primary total knee arthroplasty: a meta-analysis. *Knee surgery, sports traumatology, arthroscopy: official journal of the ESSKA*, *30*(9), 3138–3154. https://doi.org/10.1007/s00167-022-07065-5.

[69] Kim, Y. H., Park, J. W., & Jang, Y. S. (2021). Long-term result of a second or third two-stage revision total knee arthroplasty for infected total knee arthroplasty. *Arthroplasty (London, England)*, *3*(1), 8. https://doi.org/10.1186/s42836-020-00062-4.

[70] Dall'Oca, C., Ricci, M., Vecchini, E., Giannini, N., Lamberti, D., Tromponi, C., & Magnan, B. (2017). Evolution of TKA design. *Acta bio-medica: Atenei Parmensis*, *88*(2S), 17–31. https://doi.org/10.23750/abm.v88i2-S.6508.

[71] Guo, E. W., Sayeed, Z., Padela, M. T., Qazi, M., Zekaj, M., Schaefer, P., & Darwiche, H. F. (2018). Improving Total Joint Replacement with Continuous Quality Improvement Methods and Tools. *The Orthopedic clinics of North America*, *49*(4), 397–403. https://doi.org/10.1016/j.ocl.2018.05.002.

[72] Ibrahim, M. S., Alazzawi, S., Nizam, I., & Haddad, F. S. (2013). An evidence-based review of enhanced recovery interventions in knee replacement surgery. *The Annals of The Royal College of Surgeons of England*, *95*(6), 386-389.

[73] Gao, J., Xing, D., Dong, S., & Lin, J. (2020). The primary total knee arthroplasty: a global analysis. *Journal of orthopaedic surgery and research*, *15*, 1-12.

[74] Jones, R. E., Russell, R. D., & Huo, M. H. (2012). Alternatives to revision total knee arthroplasty. *The Journal of bone and joint surgery. British volume*, *94*(11 Suppl A), 137–140. https://doi.org/10.1302/0301-620X.94B11.30620.

[75] Postler, A., Lützner, C., Beyer, F., Tille, E., & Lützner, J. (2018). Analysis of Total Knee Arthroplasty revision causes. *BMC musculoskeletal disorders*, *19*(1), 55. https://doi.org/10.1186/s12891-018-1977-y.

[76] Erdemir, A., Guess, T. M., Halloran, J., Tadepalli, S. C., & Morrison, T. M. (2012). Considerations for reporting finite element analysis studies in biomechanics. *Journal of biomechanics*, *45*(4), 625–633. https://doi.org/10.1016/j.jbiomech.2011.11.038.

[77] https://www.adlerortho.com/tri-por/.

[78] https://www.adlerortho.com/tecnologia-delle-polveri/?lang=en.

[79] https://www.adlerortho.com/impianti-custom/?lang=en.

[80] Gong, X., Anderson, T., & Chou, K. (2012, June). Review on powder-based electron beam additive manufacturing technology. In *International Symposium on Flexible Automation* (Vol. 45110, pp. 507-515). American Society of Mechanical Engineers.

[81] Djoudi, F. (2013). 3D reconstruction of bony elements of the knee joint and finite element analysis of total knee prosthesis obtained from the reconstructed model. *journal of orthopaedics*, *10*(4), 155-161.

[82] Jayanthi Parthasarathy, Binil Starly, Shivakumar Raman, Andy Christensen, Mechanical evaluation of porous titanium (Ti6Al4V) structures with electron beam melting (EBM), Journal of the Mechanical Behavior of Biomedical Materials, Volume 3, Issue 3, 2010, Pages 249-259, ISSN 1751-6161, https://doi.org/10.1016/j.jmbbm.2009.10.006.

[83] Sahoo, S. (2014). Microstructure simulation of Ti-6Al-4V biomaterial produced by electron beam additive manufacturing process. *International Journal of Nano and Biomaterials*, *5*(4), 228-235.

[84] Chu, S., Guo, C., Zhang, T. *et al.* Phase-field simulation of microstructure evolution in electron beam additive manufacturing. *Eur. Phys. J. E* 43, 35 (2020). https://doi.org/10.1140/epje/i2020-11952-1.

[85] Manmeet Kaur, K. Singh, Review on titanium and titanium based alloys as biomaterials for orthopaedic applications, Materials Science and Engineering: C, Volume 102, 2019, Pages 844-862, ISSN 0928-4931, https://doi.org/10.1016/j.msec.2019.04.064.

[86] Teichtahl, A. J., Wluka, A. E., Wijethilake, P., Wang, Y., Ghasem-Zadeh, A., & Cicuttini, F. M. (2015). Wolff's law in action: a mechanism for early knee osteoarthritis. *Arthritis research & therapy*, *17*(1), 207. https://doi.org/10.1186/s13075-015-0738-7.

[87] Mi, Z. R., Shuib, S., Hassan, A. Y., Shorki, A. A., & Ibrahim, M. M. (2007). Problem of stress shielding and improvement to the hip Implat designs: A review. *J. Med. Sci*, *7*(3), 460-467.

[88] Skouras, A. Z., Kanellopoulos, A. K., Stasi, S., Triantafyllou, A., Koulouvaris, P., Papagiannis, G., & Papathanasiou, G. (2022). Clinical Significance of the Static and Dynamic Q-angle. *Cureus*, *14*(5), e24911. https://doi.org/10.7759/cureus.24911.